

CERN-TH/2003-260  
 TUM-HEP-532/03  
 FERMILAB-Pub-03/046-T  
 UCSD/PTH 03-19  
 IPPP/03/77

# Complete NNLO QCD Analysis of $\bar{B} \rightarrow X_s \ell^+ \ell^-$ and Higher Order Electroweak Effects

Christoph Bobeth<sup>a,d</sup>, Paolo Gambino<sup>b,e</sup>, Martin Gorbahn<sup>a,f</sup>,  
 and Ulrich Haisch<sup>c</sup>

<sup>a</sup> *Physik Department, Technische Universität München, D-85748 Garching, Germany*

<sup>b</sup> *Theory Division, CERN, CH-1211 Geneve 23, Switzerland*

<sup>c</sup> *Theoretical Physics Department, Fermilab, Batavia, IL 60510, USA*

<sup>d</sup> *Physics Department, University of California at San Diego, La Jolla, CA 92093, USA*

<sup>e</sup> *INFN, Sezione di Torino, 10125 Torino, Italy*

<sup>f</sup> *IPPP, Physics Department, University of Durham, DH1 3LE, Durham, UK*

## Abstract

We complete the next-to-next-to-leading order QCD calculation of the branching ratio for  $\bar{B} \rightarrow X_s \ell^+ \ell^-$  including recent results for the three-loop anomalous dimension matrix and two-loop matrix elements. These new contributions modify the branching ratio in the low- $q^2$  region,  $\text{BR}_{\ell\ell}$ , by about +1% and -4%, respectively. We furthermore discuss the appropriate normalization of the electromagnetic coupling  $\alpha$  and calculate the dominant higher order electroweak effects, showing that, due to accidental cancellations, they change  $\text{BR}_{\ell\ell}$  by only -1.5% if  $\alpha(\mu)$  is normalized at  $\mu = O(m_b)$ , while they shift it by about -8.5% if one uses a high scale normalization  $\mu = O(M_W)$ . The position of the zero of the forward-backward asymmetry,  $q_0^2$ , is changed by around +2%. After introducing a few additional improvements in order to reduce the theoretical error, we perform a comprehensive study of the uncertainty. We obtain  $\text{BR}_{\ell\ell}(1 \text{ GeV}^2 \leq q^2 \leq 6 \text{ GeV}^2) = (1.57 \pm 0.16) \times 10^{-6}$  and  $q_0^2 = (3.76 \pm 0.33) \text{ GeV}^2$  and note that the part of the uncertainty due to the  $b$ -quark mass can be easily reduced.

# 1 Introduction

The rare semileptonic  $b \rightarrow s\ell^+\ell^-$  transitions have been recently observed for the first time by Belle and BaBar in form of the exclusive  $\bar{B} \rightarrow K^{(*)}\ell^+\ell^-$  modes [1], and also inclusive measurements are now available [2]. Like all other flavor-changing-neutral-current transitions, these channels are important probes of short-distance physics. Their study can yield useful complementary information, when confronted with the less rare  $b \rightarrow s\gamma$  decays, in testing the flavor sector of the Standard Model (SM). In particular, a precise measurement of the inclusive  $\bar{B} \rightarrow X_s\ell^+\ell^-$  channel would be welcome in view of new physics searches, because it is amenable to a clean theoretical description, especially for dilepton invariant masses,  $m_{\ell\ell}^2 \equiv q^2$ , below the charm resonances, namely in the range  $1 \text{ GeV}^2 \lesssim m_{\ell\ell}^2 \lesssim 6 \text{ GeV}^2$ . In theoretical calculations the reference window is usually  $0.05 \leq \hat{s} \equiv m_{\ell\ell}^2/m_b^2 \leq 0.25$ .

The SM calculation of the Branching Ratio for  $\bar{B} \rightarrow X_s\ell^+\ell^-$  in this low- $\hat{s}$  region,  $\text{BR}_{\ell\ell}$  in the following, has reached a high degree of maturity [3–6]: it now includes a nearly complete resummation of large QCD logarithms  $L \equiv \ln m_b/M_W$  up to Next-to-Next-to-Leading Order (NNLO). The peculiarity of the  $b \rightarrow s\ell^+\ell^-$  amplitude is that it involves large logarithms even in the absence of QCD interactions. Factoring out  $G_\mu\alpha$ , it receives contributions of  $O(\alpha_s^n L^{n+1})$  at Leading Order (LO), of  $O(\alpha_s^n L^n)$  at Next-to-Leading Order (NLO), and of  $O(\alpha_s^n L^{n-1})$  at NNLO. Since the QCD penguin operators  $Q_3$ – $Q_6$  are suppressed by small Wilson coefficients, which makes the computation of their two-loop matrix elements dispensable<sup>1</sup>, the only potentially relevant NNLO terms still missing at low  $\hat{s}$  originate from the three-loop Anomalous Dimension Matrix (ADM) of the operators in the low-energy effective Hamiltonian, and from the two-loop matrix element of one of them, namely the vector-like semileptonic operator  $Q_9$ . Finally we would also like to remark that the NNLO matrix elements of the current-current operators  $Q_1$  and  $Q_2$  for the interesting high- $\hat{s}$  tail of the  $\bar{B} \rightarrow X_s\ell^+\ell^-$  decay distributions have been calculated just recently [8].

On the other hand, electroweak effects in  $b \rightarrow s\ell^+\ell^-$  have never been studied in the literature. As shown in the case of radiative decays [9–11], they may be as important as the higher order QCD effects.  $\text{BR}_{\ell\ell}$  is generally parameterized in terms of the electromagnetic coupling  $\alpha$ , but the scale at which  $\alpha$  should be evaluated is, in principle, undetermined until higher order electroweak effects are taken into account. This has led most authors to use  $\alpha(m_{\ell\ell}) \approx \alpha(m_b) \approx 1/133$ . Indeed, as we will discuss later on, in the absence of an  $O(\alpha)$  calculation, there is no reason to consider  $\alpha(m_{\ell\ell})$  more appropriate than, say,  $\alpha(M_W) \approx 1/128$ . As  $\text{BR}_{\ell\ell}$  is proportional to  $\alpha^2$ , the ensuing uncertainty of almost 8% is not at all negligible.

The purpose of this paper is threefold: *i*) in Section 2 we evaluate the two main missing NNLO QCD contributions to  $\bar{B} \rightarrow X_s\ell^+\ell^-$  taking advantage of the new results for the three-loop ADM [12, 13] and of existing calculations of  $O(\alpha_s^2)$  corrections to semileptonic

---

<sup>1</sup>In  $\bar{B} \rightarrow X_s\gamma$  the two-loop matrix elements of  $Q_3$ – $Q_6$  reduce the branching ratio by around 1% [7].

quark decays; *ii*) in Section 3 we study to what extent higher order electroweak effects influence this decay mode by calculating the dominant  $O(\alpha)$  contributions to the running of the Wilson coefficients and estimating other potentially large effects; *iii*) in Section 4 we update the SM prediction of  $\text{BR}_{\ell\ell}$  and of the position of the zero of the Forward-Backward (FB) asymmetry,  $\hat{s}_0$ , using the above results, and discuss a few improvements aimed at reducing the residual theoretical error in those observables.

## 2 Completing the NNLO QCD Calculation

Let us first focus on the missing NNLO QCD contributions. The main steps of the NNLO calculation have been outlined in [3], while two-loop matrix elements and bremsstrahlungs corrections have been computed in [4]. In the following we adopt the operator basis of [3], which we enlarge to include the electroweak penguin operators  $Q_3^Q$ – $Q_6^Q$  and the operator  $Q_1^b$ , in view of our subsequent discussion of electroweak effects:

$$\begin{aligned}
Q_1 &= (\bar{s}_L \gamma_\mu T^a c_L)(\bar{c}_L \gamma^\mu T^a b_L), & Q_2 &= (\bar{s}_L \gamma_\mu c_L)(\bar{c}_L \gamma^\mu b_L), \\
Q_3 &= (\bar{s}_L \gamma_\mu b_L) \sum_q (\bar{q} \gamma^\mu q), & Q_4 &= (\bar{s}_L \gamma_\mu T^a b_L) \sum_q (\bar{q} \gamma^\mu T^a q), \\
Q_5 &= (\bar{s}_L \gamma_\mu \gamma_\nu \gamma_\rho b_L) \sum_q (\bar{q} \gamma^\mu \gamma^\nu \gamma^\rho q), & Q_6 &= (\bar{s}_L \gamma_\mu \gamma_\nu \gamma_\rho T^a b_L) \sum_q (\bar{q} \gamma^\mu \gamma^\nu \gamma^\rho T^a q), \\
Q_3^Q &= (\bar{s}_L \gamma_\mu b_L) \sum_q Q_q (\bar{q} \gamma^\mu q), & Q_4^Q &= (\bar{s}_L \gamma_\mu T^a b_L) \sum_q Q_q (\bar{q} \gamma^\mu T^a q), \\
Q_5^Q &= (\bar{s}_L \gamma_\mu \gamma_\nu \gamma_\rho b_L) \sum_q Q_q (\bar{q} \gamma^\mu \gamma^\nu \gamma^\rho q), & Q_6^Q &= (\bar{s}_L \gamma_\mu \gamma_\nu \gamma_\rho T^a b_L) \sum_q Q_q (\bar{q} \gamma^\mu \gamma^\nu \gamma^\rho T^a q), \\
Q_1^b &= -\frac{1}{3}(\bar{s}_L \gamma_\mu b_L)(\bar{b} \gamma^\mu b) + \frac{1}{12}(\bar{s}_L \gamma_\mu \gamma_\nu \gamma_\rho b_L)(\bar{b} \gamma^\mu \gamma^\nu \gamma^\rho b), \\
Q_7 &= \frac{e}{g_s^2} m_b (\bar{s}_L \sigma^{\mu\nu} b_R) F_{\mu\nu}, & Q_8 &= \frac{1}{g_s} m_b (\bar{s}_L \sigma^{\mu\nu} T^a b_R) G_{\mu\nu}^a, \\
Q_9 &= \frac{e^2}{g_s^2} (\bar{s}_L \gamma_\mu b_L) \sum_\ell (\bar{\ell} \gamma^\mu \ell), & Q_{10} &= \frac{e^2}{g_s^2} (\bar{s}_L \gamma_\mu b_L) \sum_\ell (\bar{\ell} \gamma^\mu \gamma_5 \ell).
\end{aligned} \tag{1}$$

The operator  $Q_1^b$  corresponds in four dimensions to  $(\bar{s}_L \gamma^\mu b_L)(\bar{b}_L \gamma_\mu b_L)$  and receives contributions from electroweak boxes [14]. In order to avoid the introduction of traces with  $\gamma_5$  at all orders in QCD, we have rewritten this operator in a slightly more involved form<sup>2</sup>.

The renormalization scale dependence of the Wilson coefficients  $\vec{C}^T(\mu) = (C_1(\mu), \dots, C_{10}(\mu))$  of the effective operators is governed by the Renormalization Group Equation (RGE) whose solution is schematically given by

$$\vec{C}(\mu) = \hat{U}(\mu, \mu_0, \alpha) \vec{C}(\mu_0). \tag{2}$$

In the case at hand we are interested in the running of the Wilson coefficients from the electroweak scale  $\mu_0 = O(M_w)$  down to the low-energy scale  $\mu_b = O(m_b)$ . Neglecting for the moment the electromagnetic coupling  $\alpha$ , all the QCD corrections to the initial Wilson coefficients relevant at NNLO have explicitly been given in [3], while the only

<sup>2</sup>We thank M. Misiak for this suggestion.

$i$	1	2	3	4	5	6	7	8	9
$a_i$	$\frac{6}{23}$	$-\frac{12}{23}$	0.4086	-0.4230	-0.8994	0.1456	-1	$-\frac{24}{23}$	$\frac{3}{23}$
$b_i$	12.4592	0.6940	-1.7339	1.2360	-0.1921	0.3998	0	0	0
$c_i$	-2.5918	-0.2971	-0.5949	0.1241	0.3170	2.8655	0	0	0
$d_i$	1.3210	3.1616	-0.4814	1.9362	-5.0873	0.0468	-13.5825	0	0
$e_i$	-0.0238	0.0107	0.0023	0.0071	0.0050	-0.00003	-0.0087	-0.0008	0.0342
$f_i$	0.0010	0.0130	0.0045	-0.0022	-0.0714	-0.0008	0.0299	0	0
$g_i$	0	0	0	0	0	0	0.0035	0	0
$h_i$	0.0114	-0.0107	-0.0012	-0.0057	-0.0098	0.0002	0.0122	0	0

Table 1: Numerical coefficients parameterizing the RGE solutions in Eqs. (3), (11) and (12).

$O(\alpha_s^2)$  contributions to the evolution matrix  $\hat{U}(\mu, \mu_0, \alpha)$  pertinent to  $b \rightarrow sl^+l^-$  at NNLO concerns the mixing of  $Q_2$  into  $Q_7$  and  $Q_9$ . Expanding  $\hat{U}(\mu, \mu_0, \alpha)$  in powers of  $\alpha_s(\mu_b)/4\pi$  — see Eq. (6) — we denote these terms by  $U_{s,72}^{(2)}(\mu_b, \mu_0)$  and  $U_{s,92}^{(2)}(\mu_b, \mu_0)$ , respectively<sup>3</sup>. The ingredients necessary for the calculation of  $U_{s,72}^{(2)}(\mu_b, \mu_0)$  were already available four years ago, and are included in [3]. On the other hand, the calculation of  $U_{s,92}^{(2)}(\mu_b, \mu_0)$  requires the knowledge of the three-loop self-mixing of  $Q_1$ – $Q_6$  as well as the three-loop mixing of  $Q_1$ – $Q_6$  into  $Q_9$ . The relevant ADM entries have been calculated only recently in [12, 13]. Solving the NNLO RGE [13, 15], we obtain

$$U_{s,92}^{(2)}(\mu_b, \mu_0) = \sum_{i=1}^9 [b_i \eta^{a_i} + c_i \eta^{a_i+1} + d_i \eta^{a_i+2}] \approx 181.42 e^{-5.1901\eta} \eta^{1.5212}, \quad (3)$$

where  $\eta = \alpha_s(\mu_0)/\alpha_s(\mu_b)$ , and the so-called magic numbers  $a_i$ ,  $b_i$ ,  $c_i$  and  $d_i$  can be found in Table 1. Using  $\alpha_s(M_Z) = 0.119$  and  $m_b = 4.8$  GeV, we find numerically  $U_{s,92}^{(2)}(m_b, M_W) \approx 4.1$ . Unless  $\eta < 0.48$ , our result is within the range that was guessed in [3],  $-10\eta \leq U_{s,92}^{(2)}(\mu_b, \mu_0) \leq 10\eta$ . Our determination of  $U_{s,92}^{(2)}(\mu_b, \mu_0)$  eliminates one source of uncertainty in the NNLO calculation — we will study the residual scale dependence later on — and increases the value of  $\text{BR}_{\ell\ell}$  presented in Section 4 by about 1%, the exact amount depending on the choice of the various renormalization scales.

Another missing ingredient of the complete NNLO calculation is the two-loop  $O(\alpha_s^2)$  matrix element of  $Q_9$ . This contribution is necessary because  $Q_9$  has a non-vanishing matrix element at tree-level as well as a non-zero Wilson coefficient in leading logarithmic approximation. Fortunately, no explicit calculation is necessary in this case as the QCD corrections to  $b \rightarrow sl^+l^-$  are identical to those to  $b \rightarrow ul\nu$  ( $t \rightarrow bl\nu$ ), in the limit of vanishing strange (bottom) quark mass. In particular, we want to have the QCD corrections

<sup>3</sup>The definition of  $U_{92}^{c(2)}(\mu_b, \mu_0)$  adopted in Eq. (37) of Ref. [3] corresponds to  $\eta U_{s,92}^{(2)}(\mu_b, \mu_0)$  used here.

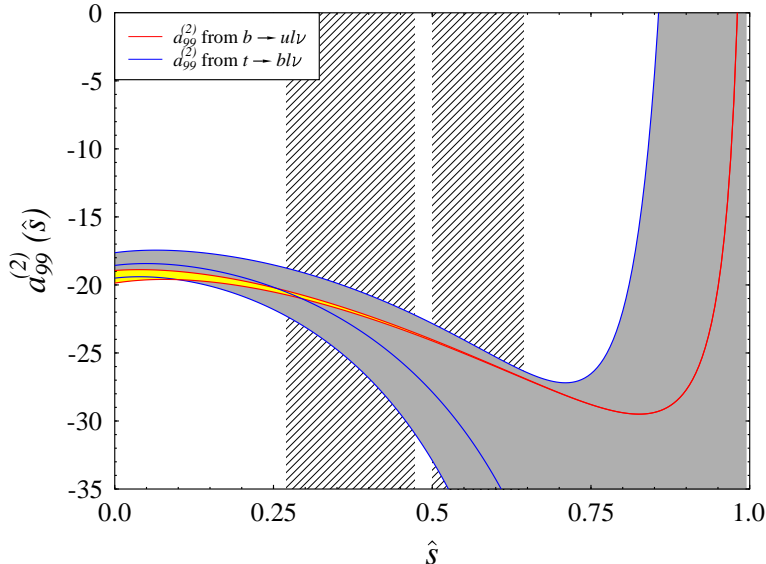


Figure 1: Second order perturbative corrections to the matrix element of  $Q_9$ , see Eq. (4), as a function of the dilepton invariant mass. The lower (upper) red curve corresponds to the  $1 - \hat{s}$  expansion up to third (fourth) order [16], while the blue curves correspond to the  $\hat{s}$  expansion [17] (central value and linearly added errors). The shaded areas show the cuts of the experimental analysis of the Belle and BaBar Collaborations [2] to reject backgrounds due to  $J/\psi$  resonances.

to the dilepton invariant mass spectrum. The  $O(\alpha_s^2)$  corrections to this spectrum for the decay  $b \rightarrow ul\nu$  have been computed in [16] in terms of an expansion in  $1 - \hat{s}$ , which converges also well in the low- $\hat{s}$  region of interest. The results up to third and fourth order in the  $1 - \hat{s}$  expansion are shown in Figure 1, in the  $b$ -quark pole mass scheme.

The dilepton invariant mass spectrum at small  $\hat{s}$  can also be obtained from the  $M_W^2/M_t^2$  expansion of the second order QCD corrections to the top quark decay calculated in [17]. In principle, using the replacements  $M_W \rightarrow m_{\ell\ell}$  and  $M_t \rightarrow m_b$ , this expansion is better suited for the low- $\hat{s}$  region. However, Ref. [17] provides only the terms up to  $M_W^4/M_t^4$ , obtained through a Padé approximation from a  $q^2/M_t^2$  expansion. The ensuing uncertainty is displayed in Figure 1, where the errors of the various coefficients have been added linearly and as before the pole mass scheme for the  $b$ -quark mass has been used. Although this is likely to overestimate the uncertainty in the calculation based on [17], the precision achieved is sufficient for our purposes. Moreover, Figure 1 shows that the two approaches [16, 17] to the calculation of the  $O(\alpha_s^2)$  corrections to the invariant dilepton mass spectrum agree

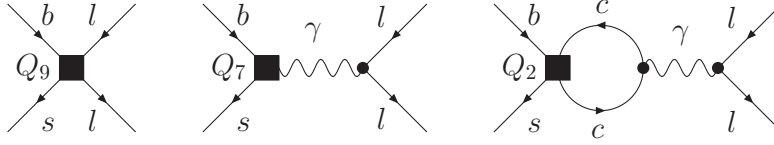


Figure 2: Some of the basic diagrams contributing to  $b \rightarrow s\ell^+\ell^-$  in the effective theory.

quite well in the low- $\hat{s}$  region. Normalizing the matrix element to its tree level value,

$$|\langle Q_9 \rangle|^2 = |\langle Q_9 \rangle^{(0)}|^2 \left[ 1 + \frac{\alpha_s(m_b)}{\pi} a_{99}^{(1)}(\hat{s}) + \left( \frac{\alpha_s(m_b)}{\pi} \right)^2 a_{99}^{(2)}(\hat{s}) \right], \quad (4)$$

a simple approximation of the real and virtual corrections denoted by  $a_{99}^{(2)}(\hat{s})$  is

$$a_{99}^{(2)}(\hat{s}) \approx -19.2 + 6.1 \hat{s} + (37.9 + 17.2 \ln \hat{s}) \hat{s}^2 - 18.7 \hat{s}^3. \quad (5)$$

This approximate formula is valid in the range  $0 \leq \hat{s} \leq 0.4$ , in the pole mass scheme for the  $b$ -quark mass. Using this expression in the NNLO calculation of  $\text{BR}_{\ell\ell}$  presented in Section 4, we observe a reduction of about 4%, that overcompensates the three-loop running of  $C_9(\mu_b)$  discussed above.

### 3 Higher Order Electroweak Effects

A comprehensive study of electroweak effects has been performed in the case of  $\bar{B} \rightarrow X_s \gamma$  [9–11] but, to the best of our knowledge, such corrections have never been considered in the calculation of  $\text{BR}_{\ell\ell}$ . Unlike in the  $b \rightarrow s\gamma$  processes, only virtual photons appear in the basic  $b \rightarrow s\ell^+\ell^-$  transition. In the following, we will try to identify and estimate the dominant  $O(\alpha)$  electroweak effects. When we consider large logarithms we refer only to terms like  $\ln m_b/M_W$  and exclude the case of very small  $\hat{s}$ , which would also involve large logarithms of the form  $\ln \hat{s}$ .

Let us first concentrate on the origin of large logarithms at  $O(\alpha)$ . To this end, it is best to work from the very beginning in the effective theory at lowest order in the electromagnetic coupling. At the weak scale, we distinguish between two kinds of contributions to the  $b \rightarrow s\ell^+\ell^-$  amplitude: *a*) those containing a virtual photon and *b*) those that do not include photons at all. Examples of the first kind are  $Q_2$  and  $Q_7$  insertions, while  $Q_9$  and  $Q_{10}$  insertions belong to the second category — see Figure 2. This classification holds true also at higher orders in QCD.

Evolving from higher to lower scales, the contributions of class *a*) receive  $O(\alpha)$  corrections involving large logarithms related either to the running of the QED coupling constant or to the evolution of the relevant Wilson coefficients. The first effect has its origin in vacuum polarization diagrams on the virtual photon propagator proportional to  $\alpha \ln m_{\ell\ell}/\mu$ , like the one shown in Figure 3, that can be effectively taken into account by changing the

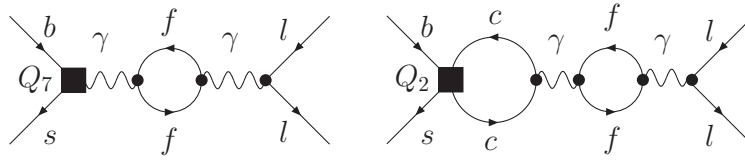


Figure 3: Vacuum polarization diagrams.

scale at which  $\alpha$  is evaluated in the overall factor of  $\text{BR}_{\ell\ell}$  from the weak scale to  $m_{\ell\ell}$ . The second effect has to do with the fact that, in full analogy to what happens in QCD, photonic interactions induce an ADM for the effective operators — see Figure 4. In order to include all  $O(\alpha)$  logarithms, it is therefore sufficient to evolve both the photonic coupling and the Wilson coefficients according to a mixed QED–QCD RGE from the matching scale  $\mu_0 = O(M_W)$  to a low-energy scale  $\mu = O(m_b)$ . Beyond leading order in  $\alpha$ , one can simply normalize the amplitudes of type *a*) with  $G_\mu\alpha(\mu)$ , and evolve the Wilson coefficients at  $\alpha$  fixed, as done in [9, 11].

Concerning contributions of class *b*), no vacuum polarization diagram can contribute at  $O(\alpha)$ , and the only  $O(\alpha)$  large logarithms are related to the running of the operators. As the normalization of the coupling constant is determined by the short distance interactions at the matching scale, the Wilson coefficients are appropriately expressed in terms of  $G_\mu$  using the relation  $g^2(M_W)/4\pi = \alpha(M_W)/\sin^2\theta_w(M_W) = \sqrt{2}/\pi G_\mu M_W^2$ , where all running couplings are in the  $\overline{\text{MS}}$  scheme. The typical case is that of box diagrams, which are clearly proportional to  $g^4(M_W)/M_W^2 \propto G_\mu^2 M_W^2$ . After decoupling, all short distance information is encoded in the Wilson coefficients and in  $G_\mu$ , which does *not* evolve in the effective theory. The coupling  $e^2$  in front of  $Q_9$  and  $Q_{10}$  — see Eq. (1) — is naturally evaluated at the weak scale.

All electroweak couplings entering the matching can be expressed in terms of  $G_\mu$ ,  $M_W$ , and  $\sin^2\theta_w(M_W)$ . These parameters are frozen in the low-energy effective theory. On the other hand, the electromagnetic coupling of the photon in the low-energy effective theory does run and the low-energy matrix elements must be expressed in terms of the low-energy gauge couplings  $\alpha_s(\mu)$  and  $\alpha(\mu)$ , and of the Wilson coefficients  $\vec{C}(\mu)$ . This simple intuitive picture is naturally realized by a mixed QED–QCD RGE. In fact, a general feature of the Renormalization Group (RG) evolution is to keep the coupling in front of the Wilson coefficients fixed at the high scale via factors of  $\alpha(\mu_0)/\alpha(\mu)$ .

The only complication we face here is due to our choice of the operator basis. The factor  $e^2/g_s^2$  in front of the operators  $Q_9$  and  $Q_{10}$  is such that the Wilson coefficients at the high scale  $C_9(\mu_0)$  and  $C_{10}(\mu_0)$  start at  $O(\alpha_s G_\mu)$  rather than at  $O(\alpha G_\mu)$ . As a consequence, the evolution of the coefficients  $C_9(\mu)$  and  $C_{10}(\mu)$  does not *explicitly* include a rescaling factor  $\alpha(\mu_0)/\alpha(\mu)$  as, for instance, in the standard QCD evolution of  $C_1(\mu)$  and  $C_2(\mu)$ . However, we will show at the end of this section that the correct normalization of the electroweak coupling in front of these contributions is preserved by the QED  $\beta$  function coefficients  $\beta_e^{(0)}$  and  $\beta_{es}^{(1)}$  that appear in the self-mixing of  $Q_9$  and  $Q_{10}$  — see Eqs. (38) and (39) — due to the  $e^2$  factor in the definition of these operators.



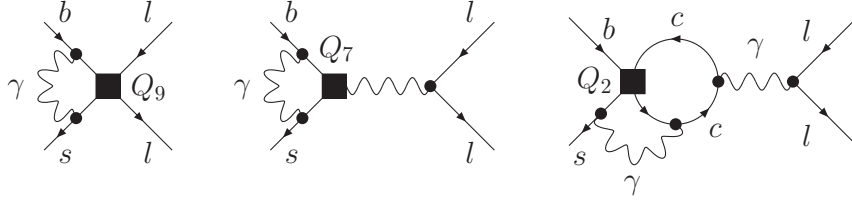


Figure 4: Some diagrams contributing to the running of the Wilson coefficients.

Summarizing, we perform the RG evolution of the Wilson coefficients which results in the normalization of the whole amplitude in terms of  $\alpha(\mu)$ . As we will discuss later on, additional sub-dominant corrections come from  $O(\alpha)$  matrix elements of the effective operators and from  $O(\alpha)$  corrections to the matching conditions. We employ  $\sin^2 \theta_w \equiv \sin^2 \hat{\theta}_w^{\overline{\text{MS}}}(M_Z) = 0.2312$ ,  $M_t = M_t(M_t) = 165 \text{ GeV}$  and  $M_W = 80.426 \text{ GeV}$ . We adopt an  $\overline{\text{MS}}$  definition of  $\alpha(\mu)$  with  $\alpha^{(5)}(M_Z) = 1/127.765$  [19] as input.

Let us now study explicitly the QED–QCD evolution of the Wilson coefficients. Our basis (1) differs from the one used in [9] by a factor  $g_s^{-2}$  in the normalization of  $Q_7$ – $Q_{10}$ , which complicates slightly the counting of couplings and the comparison with the latter paper. Neglecting the running of  $\alpha$  — an  $O(\alpha^2)$  effect in the running of the Wilson coefficients — we can expand the evolution matrix  $\hat{U}(\mu, \mu_0, \alpha)$  of Eq. (2) in the following way

$$\begin{aligned} \hat{U}(\mu, \mu_0, \alpha) = & \hat{U}_s^{(0)}(\mu, \mu_0) + \frac{\alpha_s(\mu)}{4\pi} \hat{U}_s^{(1)}(\mu, \mu_0) + \left( \frac{\alpha_s(\mu)}{4\pi} \right)^2 \hat{U}_s^{(2)}(\mu, \mu_0) \\ & + \frac{\alpha}{\alpha_s(\mu)} \hat{U}_e^{(0)}(\mu, \mu_0) + \frac{\alpha}{4\pi} \hat{U}_e^{(1)}(\mu, \mu_0) + \frac{\alpha\alpha_s(\mu)}{(4\pi)^2} \hat{U}_e^{(2)}(\mu, \mu_0) + \dots \end{aligned} \quad (6)$$

The matrices  $\hat{U}_s^{(i)}(\mu, \mu_0)$  and  $\hat{U}_e^{(i)}(\mu, \mu_0)$  describe pure QCD and mixed QED–QCD evolution, respectively, and are functions of the ADM<sup>4</sup>

$$\begin{aligned} \hat{\gamma}(\mu) = & \frac{\alpha_s(\mu)}{4\pi} \hat{\gamma}_s^{(0)} + \left( \frac{\alpha_s(\mu)}{4\pi} \right)^2 \hat{\gamma}_s^{(1)} + \left( \frac{\alpha_s(\mu)}{4\pi} \right)^3 \hat{\gamma}_s^{(2)} \\ & + \frac{\alpha}{4\pi} \hat{\gamma}_e^{(0)} + \frac{\alpha\alpha_s(\mu)}{(4\pi)^2} \hat{\gamma}_e^{(1)} + \dots, \end{aligned} \quad (7)$$

of the operators in question and of the QCD, QED and mixed QED–QCD  $\beta$  functions. The matrices  $\hat{U}_e^{(0)}(\mu, \mu_0)$  and  $\hat{U}_e^{(1)}(\mu, \mu_0)$  can be computed using the formalism described for instance in [20]. Expanding also the Wilson coefficients at the weak scale

$$\begin{aligned} \vec{C}(\mu_0) = & \vec{C}_s^{(0)}(\mu_0) + \frac{\alpha_s(\mu_0)}{4\pi} \vec{C}_s^{(1)}(\mu_0) + \left( \frac{\alpha_s(\mu_0)}{4\pi} \right)^2 \vec{C}_s^{(2)}(\mu_0) \\ & + \frac{\alpha}{4\pi} \vec{C}_e^{(1)}(\mu_0) + \frac{\alpha\alpha_s(\mu_0)}{(4\pi)^2} \vec{C}_e^{(2)}(\mu_0) + \dots, \end{aligned} \quad (8)$$

<sup>4</sup>Eq. (7) contains also a term proportional to  $\alpha^2/\alpha_s(\mu)$ , from the mixing of  $Q_9$  into  $Q_3^Q$ . We have checked that its contribution to the evolution of the relevant Wilson coefficients is negligibly small.



and inserting (6) and (8) into (2), we find the expressions for the various terms at the low scale  $\mu$

$$\begin{aligned} \vec{C}(\mu) &= \vec{C}_s^{(0)}(\mu) + \frac{\alpha_s(\mu)}{4\pi} \vec{C}_s^{(1)}(\mu) + \left(\frac{\alpha_s(\mu)}{4\pi}\right)^2 \vec{C}_s^{(2)}(\mu) \\ &+ \frac{\alpha}{\alpha_s(\mu)} \vec{C}_e^{(0)}(\mu) + \frac{\alpha}{4\pi} \vec{C}_e^{(1)}(\mu) + \frac{\alpha\alpha_s(\mu)}{(4\pi)^2} \vec{C}_e^{(2)}(\mu) + \dots \end{aligned} \quad (9)$$

Here the coefficients  $\vec{C}_s^{(i)}(\mu)$  result from the  $O(1)$ ,  $O(\alpha_s)$  and  $O(\alpha_s^2)$  contributions to  $\vec{C}(\mu_0)$  and from the QCD evolution matrices  $\hat{U}_s^{(i)}(\mu, \mu_0)$ , whereas the  $\vec{C}_e^{(i)}(\mu)$  stem from the various  $O(\alpha)$  corrections to  $\vec{C}(\mu_0)$  and the QCD, QED–QCD evolution matrices  $\hat{U}_s^{(i)}(\mu, \mu_0)$  and  $\hat{U}_e^{(i)}(\mu, \mu_0)$ .

The formally leading electroweak effects are  $O(\alpha\alpha_s^{n-1}L^{n+1})$  in the amplitude and are contained in

$$\vec{C}_e^{(0)}(\mu) = \hat{U}_e^{(0)}(\mu, \mu_0) \vec{C}_s^{(0)}(\mu_0). \quad (10)$$

The non-vanishing  $O(\alpha)$  mixing described by  $\hat{\gamma}_e^{(0)}$  has been calculated in [10], except for the QED mixing of  $Q_9$  and  $Q_{10}$ . The lowest order —  $O(\alpha_s)$  in our notation — mixing between the electroweak penguin operators  $Q_3^Q$ – $Q_6^Q$  and  $Q_9$  is also missing in the literature, as is the  $O(\alpha_s)$  mixing of the operator  $Q_1^b$ . We have computed all missing entries and report the full matrices  $\hat{\gamma}_e^{(0)}$  and  $\hat{\gamma}_s^{(0)}$  in the Appendix. Since only the mixing of  $Q_2$  into  $Q_9$  and  $Q_{10}$  is relevant at this order, we solve the RGE and get

$$C_{e,9}^{(0)}(\mu) = \sum_{i=1}^9 [e_i \eta^{a_i-1} + f_i \eta^{a_i}] \approx 5.7947 e^{-11.508\eta} \eta^{2.8808}, \quad (11)$$

where we used  $C_2^{(0)}(\mu_0) = 1$ , and the magic numbers  $a_i$ ,  $e_i$  and  $f_i$  are given in Table 1. The approximation is valid within less than 1% for  $0.5 \leq \eta \leq 0.6$ . The formally leading QED contribution shifts  $C_9(m_b)$  by only 0.00006 for  $\eta = 0.56$ . Since  $Q_9$  mixes into  $Q_{10}$  at  $O(\alpha)$  we also have a contribution to

$$C_{e,10}^{(0)}(\mu) = \sum_{i=1}^9 [g_i \eta^{a_i-1} + h_i \eta^{a_i}] \approx 1.9013 e^{-9.7876\eta} \eta^{1.2089}, \quad (12)$$

which shifts  $C_{10}(m_b)$  by 0.00014 for  $\eta = 0.56$ . Again the numerical coefficients  $a_i$ ,  $g_i$  and  $h_i$  can be found in Table 1, and the approximation is valid within less than 1% for  $0.5 \leq \eta \leq 0.6$ . Since in our normalization  $C_9(m_b) \simeq 0.072$  and  $C_{10}(m_b) \simeq -0.072$  at NNLO QCD, the impact of these  $O(\alpha/\alpha_s)$  corrections on  $\text{BR}_{\ell\ell}$  is tiny.

As discussed in [9,21], next-to-leading electroweak effects can be larger than the leading ones. Moreover, in the case of  $b \rightarrow s\ell^+\ell^-$ , the LO QCD contribution is accidentally small compared to the NLO QCD contribution. Let us therefore investigate the importance of these  $O(\alpha\alpha_s^{n-1}L^n)$  effects. The general expression for  $\vec{C}_e^{(1)}(\mu)$  is

$$\vec{C}_e^{(1)}(\mu) = \hat{U}_s^{(0)}(\mu, \mu_0) \vec{C}_e^{(1)}(\mu_0) + \eta \hat{U}_e^{(0)}(\mu, \mu_0) \vec{C}_s^{(1)}(\mu_0) + \hat{U}_e^{(1)}(\mu, \mu_0) \vec{C}_s^{(0)}(\mu_0). \quad (13)$$

The last term in this equation requires the knowledge of the  $O(\alpha_s)$  ADM  $\hat{\gamma}_e^{(1)}$ , which we have calculated using the method described in [12]. The result is given in the Appendix. Rather than giving analytic expressions for these  $O(\alpha)$  corrections to the Wilson coefficients of  $Q_7$ ,  $Q_9$  and  $Q_{10}$ , we only provide some approximate formulas and refer to a forthcoming publication [22] for more details. Taking into account the different operator normalization, we find the same results as in [9] for the  $O(\alpha)$  correction to the Wilson coefficient of the electromagnetic operator,

$$\begin{aligned} C_{e,7}^{(1)}(\mu) &\approx 0.2894 e^{-5.1605\eta} \eta^{1.4543} x_t^{0.3060} + 10654 e^{-14.857\eta} \eta^{8.2193} \\ &\approx 0.0107 + 0.0221, \end{aligned} \quad (14)$$

where we have distinguished between the last two terms on the right-hand side of Eq. (13) — in the particular case of  $C_7(\mu)$  the first term is exactly zero as there is no  $O(\alpha_s)$  mixing of the four-quark operators into the magnetic one, and the  $O(\alpha)$  contribution to  $C_7(\mu_0)$  also vanishes in the normalization employed here, see Eq. (1). The approximate formulas given above and in the following are all valid within 1% for  $0.5 \leq \eta \leq 0.6$  and  $160 \text{ GeV} \leq M_t \leq 170 \text{ GeV}$ . Furthermore, the last line of the latter equation gives the numerical values of the individual contributions for  $\eta = 0.56$  and  $M_t(M_t) = 165 \text{ GeV}$ . All together, these  $O(\alpha)$  contributions lead to a shift of 0.00002 in  $C_7(m_b)$ . Given that in our normalization  $C_7(m_b) \simeq -0.0053$  at NNLO QCD, this correction is quite small. The analogous expression for  $C_9(\mu)$  reads

$$\begin{aligned} C_{e,9}^{(1)}(\mu) &\approx -41.496 e^{-4.8790\eta} \eta^{0.4747} x_t^{0.4738} + 75.537 e^{-5.4866\eta} \eta^{0.4931} x_t^{-1.9596} \\ &\quad + 13.565 e^{-6.0599\eta} \eta^{2.3409} \\ &\approx -4.0517 + 0.1579 + 0.1173. \end{aligned} \quad (15)$$

Here and in the following numerical results we have set  $\mu_0 = M_w$ . We have distinguished between the three terms in Eq. (13). Again, the last line in the above equation gives the numerical value of the three contributions for  $\eta = 0.56$  and  $M_t(M_t) = 165 \text{ GeV}$ : this electroweak correction to  $C_9(m_b)$  is around  $-0.00226$ , thus much larger than the one in Eq. (11). Moreover, it is dominated by the first term in Eq. (13), namely by the  $O(\alpha)$  matching conditions, and particularly by those of the electroweak penguin operators. Numerically, it corresponds to approximately  $-3\%$  of the NNLO QCD coefficient. The corresponding expression for  $C_{10}(\mu)$  is

$$\begin{aligned} C_{e,10}^{(1)}(\mu) &\approx -20.835 e^{-4.9135\eta} \eta^{0.4957} x_t^{0.8394} + 67049 e^{-15.347\eta} \eta^{8.8810} \\ &\approx -3.3340 + 0.0720. \end{aligned} \quad (16)$$

The shift in  $C_{10}(m_b)$  is about  $-0.00195$ , and is again dominated by a term stemming from the higher order matching corrections. Like in the case of  $C_7(\mu)$ , the term resulting from the leading order QCD running is exactly zero since there is no mixing of the four-quark

operators into  $Q_{10}$  at  $O(\alpha_s)$ , and the  $O(\alpha)$  correction to  $C_{10}(\mu_0)$  is zero too. Numerically, it corresponds to approximately +3% of the NNLO QCD coefficient.

The experience with radiative decays [9] shows that electroweak corrections to the matching conditions may end up being the dominant electroweak contributions to the low scale coefficients. In the notation adopted here, such contributions to  $C_7(\mu_0)$ ,  $C_9(\mu_0)$  and  $C_{10}(\mu_0)$  are of  $O(\alpha\alpha_s)$  and therefore formally enter at NNLO or  $O(\alpha\alpha_s^n L^n)$  in the  $b \rightarrow s\ell^+\ell^-$  amplitude. Although a complete analysis at this order is clearly beyond the scope of our paper, it is worth investigating the magnitude of the potentially dominant terms, such as electroweak effects in the matching enhanced by factors  $1/\sin^2\theta_w \approx 4.3$  or by powers of  $M_t$ . The general expression for  $\vec{C}_e^{(2)}(\mu)$  at the low scale is

$$\begin{aligned} \vec{C}_e^{(2)}(\mu) = & \eta \hat{U}_s^{(0)}(\mu, \mu_0) \vec{C}_e^{(2)}(\mu_0) + \eta^2 \hat{U}_e^{(0)}(\mu, \mu_0) \vec{C}_s^{(2)}(\mu_0) \\ & + \hat{U}_s^{(1)}(\mu, \mu_0) \vec{C}_e^{(1)}(\mu_0) + \eta \hat{U}_e^{(1)}(\mu, \mu_0) \vec{C}_s^{(1)}(\mu_0) + \hat{U}_e^{(2)}(\mu, \mu_0) \vec{C}_s^{(0)}(\mu_0). \end{aligned} \quad (17)$$

The second, third, and fourth term in this equation are known completely, from [3] and the above discussion. The first term is partially known: in particular  $C_{e,7}^{(2)}(\mu_0)$  and  $C_{e,8}^{(2)}(\mu_0)$  are known from [9], while only the part of  $C_{e,9}^{(2)}(\mu_0)$  and  $C_{e,10}^{(2)}(\mu_0)$  proportional to  $M_t^4$  is known from [23]. We also include in the following the leading contributions to  $C_{e,3}^{Q(2)}(\mu_0)$ – $C_{e,6}^{Q(2)}(\mu_0)$  calculated in [3, 21]<sup>5</sup>. The last term in Eq. (17) would require the knowledge of the three-loop  $O(\alpha\alpha_s^2)$  ADM and will be neglected in what follows. Again, rather than giving analytic expressions for these NNLO corrections, we will only give some approximate formulas and refer to a forthcoming publication [22] for more details. We use the results of [3, 9, 21, 23] for the  $O(\alpha\alpha_s)$  initial conditions of the relevant Wilson coefficients and find for the correction to  $C_7(\mu)$

$$\begin{aligned} C_{e,7}^{(2)}(\mu) \approx & 2.9457 e^{-0.4323\eta} \eta^{1.3783} x_t^{0.9498} + 1.2160 e^{-5.4241\eta} \eta^{2.1365} x_t^{-0.5479} \\ & - 6.8887 \times 10^{10} e^{-34.605\eta} \eta^{13.470} x_t^{0.9677} + 50.557 e^{-5.9375\eta} \eta^{2.6489} x_t^{-0.0736} \\ \approx & 4.0718 + 0.0077 - 0.4315 + 0.3522. \end{aligned} \quad (18)$$

The analogous expression for  $C_9(\mu)$  reads

$$\begin{aligned} C_{e,9}^{(2)}(\mu) \approx & 2.3684 \times 10^{11} e^{-31.006\eta} \eta^{12.546} x_t^{-0.9681} - 209.52 e^{-4.6671\eta} \eta^{2.3626} x_t^{-1.7441} \\ & + 519.80 e^{-6.5763\eta} \eta^{3.1984} x_t^{0.4666} + 94.434 e^{-4.8623\eta} \eta^{1.1723} x_t^{0.5775} \\ \approx & 1.1803 - 0.3190 + 4.0021 + 7.2083. \end{aligned} \quad (19)$$

Finally, for the  $O(\alpha\alpha_s)$  correction to  $C_{10}(\mu)$  we get

$$\begin{aligned} C_{e,10}^{(2)}(\mu) \approx & 0.3106 x_t^{2.6056} - 242.56 e^{-4.7109\eta} \eta^{1.5336} x_t^{-0.7682} \\ & + 80.747 e^{-4.9425\eta} \eta^{1.2373} x_t^{0.7343} \\ \approx & 13.144 - 2.3657 + 7.1098. \end{aligned} \quad (20)$$

---

<sup>5</sup>Since the calculation of Ref. [21] has been performed in a different operator basis one has to perform a non-trivial change of scheme. See [22] for details.

In the last equation the contribution of the third term in Eq.(17) is exactly zero. In Eqs. (18), (19) and (20) we have set  $M_H = 115$  GeV and the last line always corresponds to the numerical value of the four individual contributions to Eq. (17), employing  $\eta = 0.56$ ,  $M_t(M_t) = 165$  GeV, and setting  $\mu_0 = M_W$  and  $\mu_t = M_t$ . For what concerns  $C_7(m_b)$ , these  $O(\alpha\alpha_s)$  corrections are twice as large as the  $O(\alpha)$  correction, and lead to a shift of 0.00004. On the other hand, in the case of  $C_9(m_b)$  and  $C_{10}(m_b)$  they are much smaller than the corrections of  $O(\alpha)$ , as they amount to only 0.00016 and 0.00018. We stress that they are *incomplete* and we study them to check the potential size of the higher order contributions. If we add these partial higher order results to the complete leading and next-to-leading electroweak effects considered above, the values of the Wilson coefficients of  $Q_7$ ,  $Q_9$  and  $Q_{10}$  are changed by  $-1.1\%$ ,  $-2.9\%$  and  $+2.3\%$ , respectively.

At this point we also note that the electroweak corrections to  $C_{10}(\mu_b)$  depend rather strongly on the  $t$ -quark mass renormalization scale  $\mu_t$ . Using  $M_t(M_W) = 175$  GeV instead of  $M_t(M_t) = 165$  GeV, which usually leads to larger higher order QCD corrections, one finds a correction of  $+5.3\%$ . This scheme dependence stems from the parts of  $C_{e,10}^{(2)}(\mu_0)$  proportional to  $M_t^4$  computed in [23], which we have evaluated in the  $\overline{\text{MS}}$  scheme for the  $t$ -quark mass. On the other hand, the  $\mu_t$ -dependence of the QED corrections to  $C_7(\mu_b)$  and  $C_9(\mu_b)$  is very weak.

Let us now verify that the RGE has indeed preserved the correct normalization of the electroweak coupling for the matching contributions to  $Q_9$  and  $Q_{10}$ , as anticipated at the beginning of this section. To this end, we first consider the effect of the  $\beta_e^{(0)}$  terms in the ADM of Eq. (38). Using the explicit form of  $\hat{U}_e^{(0)}(\mu, \mu_0)$ , one sees that they modify the contribution of  $C_9(\mu_0)$  to the low-energy Wilson coefficients as follows

$$\begin{aligned}
U_{s,99}^{(0)}(\mu, \mu_0)C_9(\mu_0) &\rightarrow \left[ 1 - \alpha \frac{\beta_e^{(0)}}{\beta_s^{(0)}} \left( \frac{1}{\alpha_s(\mu)} - \frac{1}{\alpha_s(\mu_0)} \right) \right] U_{s,99}^{(0)}(\mu, \mu_0)C_9(\mu_0) \\
&\approx \frac{\alpha(\mu_0)}{\alpha(\mu)} U_{s,99}^{(0)}(\mu, \mu_0)C_9(\mu_0),
\end{aligned}
\tag{21}$$

where the equality holds up to small higher order terms in  $\alpha$  and up to subleading logarithms in  $\alpha_s$ . Indeed, the consideration of subleading QCD effects, like those contained in  $\hat{U}_e^{(1)}(\mu, \mu_0)$ , shows that QCD does not affect the proper normalization of the electroweak coupling, as anticipated above. Equation (21) and the analogous relation for  $C_{10}(\mu_0)$  demonstrate that the physically motivated normalization of the electroweak coupling is preserved by the RG evolution even for our choice of normalization of the operators: since the matrix element is multiplied by  $\alpha(\mu)$ , the rescaling factor in front of  $C_9(\mu_0)$  brings the normalization of the electromagnetic coupling back to the electroweak scale. All other large logarithms described by the QED–QCD evolution matrices  $\hat{U}_e^{(i)}(\mu, \mu_0)$  are solely induced by the running of the operators.

While  $\hat{U}_s^{(0)}(\mu, \mu_0)$  and  $\hat{U}_e^{(0)}(\mu, \mu_0)$  are scheme-independent,  $\hat{U}_s^{(1)}(\mu, \mu_0)$  and  $\hat{U}_e^{(1)}(\mu, \mu_0)$  depend on the renormalization scheme in a way that is detailed for example in Ref. [21].

The scheme dependence is canceled by the  $O(\alpha_s)$  and  $O(\alpha)$  matrix elements of the effective operators. In fact, any calculation that goes beyond leading logarithms requires the knowledge of the one-loop matrix elements. However, we have seen above that the dominant effects originate at the weak scale and have often to do with  $O(\alpha/\sin^2\theta_w)$  contributions to the matching conditions. These contributions are all scheme-independent. One could also absorb some contributions to the QED matrix elements by replacing  $\alpha(\mu)$  with  $\alpha(m_{\ell\ell})$ , as discussed at the beginning of this section. However, numerically this would lead to a small difference and we will avoid it. We therefore expect our incomplete calculation to capture the dominant electroweak effects. Moreover, any complete calculation of the QED matrix elements should take into account real photon radiation, which is very sensitive to the details of the experimental set-up and requires a dedicated study at the experimental level.

## 4 Phenomenology

We are now ready to combine all our results and update the prediction for  $\text{BR}_{\ell\ell}$ . We first write the integrated branching ratio as in [3, 4]:

$$\text{BR}_{\ell\ell} = \text{BR}[\bar{B} \rightarrow X_c \ell \nu] \int_{0.05}^{0.25} d\hat{s} \frac{1}{\Gamma[\bar{B} \rightarrow X_c \ell \nu]} \frac{d\Gamma[\bar{B} \rightarrow X_s \ell^+ \ell^-]}{d\hat{s}}, \quad (22)$$

where

$$\begin{aligned} \frac{d\Gamma[\bar{B} \rightarrow X_s \ell^+ \ell^-]}{d\hat{s}} = & \frac{G_\mu^2 m_{b,\text{pole}}^5 |V_{ts}^* V_{tb}|^2}{48\pi^3} \left(\frac{\alpha(m_b)}{4\pi}\right)^2 (1-\hat{s})^2 \left\{ \left(4 + \frac{8}{\hat{s}}\right) \left|\tilde{C}_{7,\text{BR}}^{\text{eff}}(\hat{s})\right|^2 \right. \\ & \left. + (1+2\hat{s}) \left( \left|\tilde{C}_{9,\text{BR}}^{\text{eff}}(\hat{s})\right|^2 + \left|\tilde{C}_{10,\text{BR}}^{\text{eff}}(\hat{s})\right|^2 \right) + 12 \text{Re} \left( \tilde{C}_{7,\text{BR}}^{\text{eff}}(\hat{s}) \tilde{C}_{9,\text{BR}}^{\text{eff}}(\hat{s})^* \right) + \frac{d\Gamma^{\text{Brems}}}{d\hat{s}} \right\}, \end{aligned} \quad (23)$$

and the effective Wilson coefficients include all real and virtual QCD corrections [4] as indicated by the index BR, whereas the last term encodes finite bremsstrahlungs corrections computed in the second paper of Ref. [4]. At  $O(\alpha)$  the definition of the effective Wilson coefficients is affected by the presence of the electroweak penguin operators  $Q_3^Q - Q_6^Q$  and of  $Q_1^b$  — for a detailed discussion we refer to [22]. In order to cancel the strong dependence on the bottom quark mass in the factor  $m_b^5$ , it is customary to normalize  $\text{BR}_{\ell\ell}$  to the experimental value of the Branching Ratio (BR) for the inclusive semileptonic decay  $\text{BR}[\bar{B} \rightarrow X_c \ell \nu]$ . However, this normalization introduces a strong dependence on the charm quark mass, which is not known very accurately. The ensuing uncertainty is about 8% [5]. An alternative procedure [25, 26] consists in normalizing the  $\bar{B} \rightarrow X_s \ell^+ \ell^-$  decay width to  $\Gamma[\bar{B} \rightarrow X_u \ell \nu]$ , and then to express  $\text{BR}[\bar{B} \rightarrow X_u \ell \nu]$  in terms of  $\text{BR}[\bar{B} \rightarrow X_c \ell \nu]$  and of the ratio

$$C = \left| \frac{V_{ub}}{V_{cb}} \right|^2 \frac{\Gamma[\bar{B} \rightarrow X_c \ell \nu]}{\Gamma[\bar{B} \rightarrow X_u \ell \nu]}, \quad (24)$$

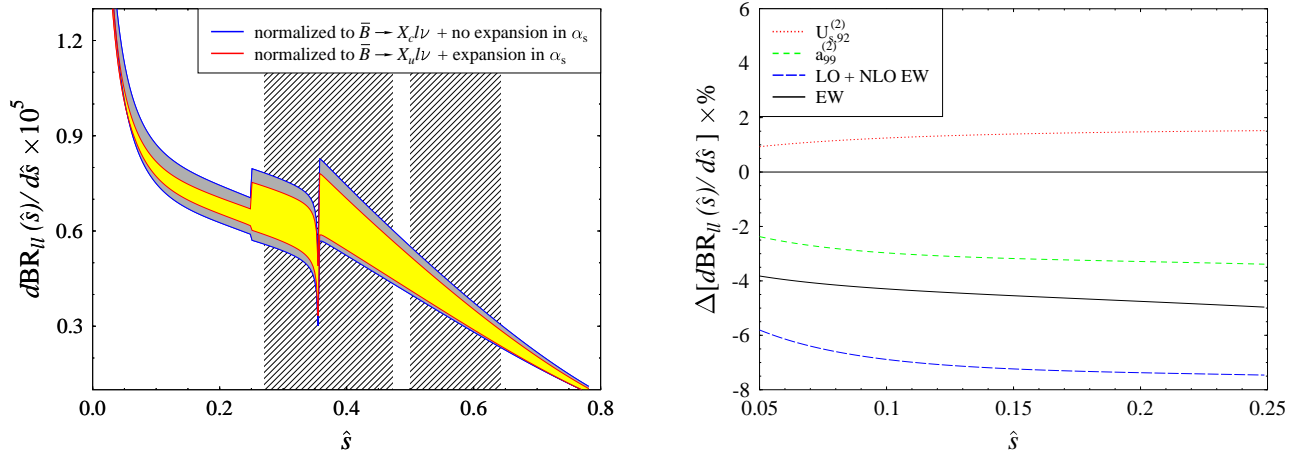


Figure 5: Scale dependence of the differential  $\text{BR}_{\ell\ell}$  using the different normalizations of Eqs. (22) and (25) in the partial NNLO QCD approximation (lhs). The discontinuity at the end of the low- $\hat{s}$  region reflects the fact that the  $O(\alpha_s^2)$  matrix elements of  $Q_1$  and  $Q_2$  have not been implemented for  $\hat{s} > 0.25$  [8], while the divergence in the  $J/\psi$  region is due to the  $1/m_c^2$  corrections. Furthermore the relative size of the NNLO and electroweak (EW) effects introduced in this paper are shown when *sequentially* included (rhs).

which can be computed with better accuracy [25]. In other words, we will use

$$\text{BR}_{\ell\ell} = \frac{\text{BR}[\bar{B} \rightarrow X_c \ell \nu]}{C} \left| \frac{V_{ub}}{V_{cb}} \right|^2 \int_{0.05}^{0.25} d\hat{s} \frac{1}{\Gamma[\bar{B} \rightarrow X_u \ell \nu]} \frac{d\Gamma[\bar{B} \rightarrow X_s \ell^+ \ell^-]}{d\hat{s}}. \quad (25)$$

The main uncertainty in  $C$  comes from non-perturbative effects. Using an updated determination of the heavy quark effective theory parameter  $\lambda_1 = (-0.31 \pm 0.10) \text{ GeV}^2$  [27], and following otherwise Ref. [25], we obtain  $C = 0.581 \pm 0.017$ . For the inclusive semileptonic  $b \rightarrow c$  branching ratio we use  $\text{BR}_{sl} \equiv \text{BR}[\bar{B} \rightarrow X_c \ell \nu] = (10.74 \pm 0.24)\%$  obtained from the latest Heavy Flavor Averaging Group results [28] after subtracting the  $b \rightarrow u$  transition. For the Cabbibo-Kobayashi-Maskawa (CKM) factor  $|V_{ts}^* V_{tb}|^2 / |V_{cb}|^2$  we use  $0.969 \pm 0.005$  [27], but we actually perform the calculation keeping top, charm and up quark sectors separated [3]. Finally, we employ the  $c$ - and  $b$ -quark pole masses,  $m_{c,\text{pole}} = (1.4 \pm 0.2) \text{ GeV}$  and  $m_{b,\text{pole}} = (4.80 \pm 0.15) \text{ GeV}$ .

The use of the  $b$ -quark pole mass in Eq. (23) and in the calculation of the semileptonic width leads to large perturbative QCD corrections both in the numerator and denominator of Eqs. (22) and (25). Since this is an artifact of the choice of scheme for the bottom quark mass, they clearly tend to cancel in the ratio. As a second improvement with respect to previous analyses, we keep terms through  $O(\alpha_s^2)$  in the denominator and expand the ratio in Eq. (25) in powers of  $\alpha_s$ . By making explicit the cancellation of large contributions, we improve the convergence and stability of the perturbative series, as we have explicitly



	partial NNLO	$U_{s,92}^{(2)}$	$a_{99}^{(2)}$	LO + NLO EW	EW
BR $_{\ell\ell}$ as in (26)	$1.509^{+0.035}_{-0.088}$	$1.529^{+0.030}_{-0.081}$	$1.463^{+0.038}_{-0.080}$	$1.403^{+0.056}_{-0.087}$	$1.442^{+0.054}_{-0.069}$
BR $_{\ell\ell}$ as in (27)	$1.646^{+0.038}_{-0.095}$	$1.668^{+0.032}_{-0.087}$	$1.597^{+0.041}_{-0.087}$	$1.532^{+0.060}_{-0.094}$	$1.574^{+0.059}_{-0.075}$

Table 2: BR $_{\ell\ell}$  integrated over the low- $\hat{s}$  and low- $q^2$  region in units  $10^{-6}$ . The different corrections are added in sequence.

checked. Like in previous analyses, due to the peculiarity of the perturbative expansion for  $b \rightarrow s\ell^+\ell^-$ , we retain some large and scheme-independent higher order term in the amplitude squared: for instance the terms  $|\tilde{C}_7^{\text{eff}}(\hat{s})|^2$  and  $|\tilde{C}_{10}^{\text{eff}}(\hat{s})|^2$  in Eq. (23) are expanded up to  $O(\alpha_s)$ . In addition all known  $O(\alpha_s)$  terms of  $|\tilde{C}_9^{\text{eff}}(\hat{s})|^2$  and  $\text{Re}(\tilde{C}_7^{\text{eff}}(\hat{s})\tilde{C}_9^{\text{eff}}(\hat{s})^*)$  are kept. Our procedure differs slightly from the one proposed in the first paper of [4], which consists in absorbing the numerically small coefficient  $C_{s,9}^{(0)}(\mu_b)$  into  $C_{s,9}^{(1)}(\mu_b)$ , and in subsequently performing the  $\alpha_s$  expansion of the numerator  $d\Gamma[\bar{B} \rightarrow X_s\ell^+\ell^-]/d\hat{s}$  only. In the partial NNLO approximation, that is, setting  $U_{s,92}^{(2)}(\mu_b, \mu_0)$  and  $a_{99}^{(2)}(\hat{s})$  to zero, this alternative method yields somewhat lower values for the normalized differential rate, well within the scale dependence of our results.

We also include power corrections of  $O(1/m_b^2)$  [29] and  $O(1/m_c^2)$  [30] to the differential decay rate of  $\bar{B} \rightarrow X_s\ell^+\ell^-$  as well as  $O(1/m_b^2)$  corrections to  $\Gamma[\bar{B} \rightarrow X_c\ell\nu]$  and  $\Gamma[\bar{B} \rightarrow X_u\ell\nu]$  — see for example [31] — and expand the normalized differential decay rates given in Eqs. (22) and (25) in inverse powers of  $m_b$  and  $m_c$ .

The partial NNLO results before inclusion of the two contributions discussed in Section 2 are shown in the left plot of Figure 5, where the bands include only the residual scale dependence, calculated performing a scan in the ranges: [40–120] GeV for the matching scale in the charm and up sector, [60–180] GeV for the matching scale in the top sector, [2.5–10] GeV for the low-energy renormalization scale. In the last case, the central value is set to 5 GeV. As can be nicely seen by comparing the gray with the yellow band, the residual scale dependence for low  $\hat{s}$  is about 50% smaller in our approach than without the two improvements introduced between Eqs. (23) and (25). On the other hand, the scale uncertainty is practically unaffected by the new NNLO contributions — not shown in Figure 5.

The results for the integrated BR are given in the first line of Table 2, where the first column refers to the partial NNLO calculation according to [4] but implemented as described above, the second column to the same calculation supplemented by our result for  $U_{s,92}^{(2)}(\mu_b, \mu_0)$ , the third column to the complete NNLO, that is, including the two-loop QCD matrix element  $a_{99}^{(2)}(\hat{s})$ . The fourth column refers to the NNLO calculation including LO and NLO electroweak effects, and the fifth column to the QCD computation supplemented by the electroweak effects through NNLO calculated in the previous section. Furthermore, in the last two columns the dominant QED corrections to the semileptonic



decay amplitude [32] have been included. If we had only rescaled the matching conditions for  $Q_9$  and  $Q_{10}$  and for the penguin operators by a factor  $\alpha(M_W)/\alpha(m_b)$  as discussed in the previous section, the shift would be close to +7%. This effect is overcompensated by other electroweak corrections of around -7% and by the QED correction to the semileptonic rate, which by itself amounts to around -1.5%. We would like to stress that this is an unexpected accidental cancellation. The right plot of Figure 5 shows  $\Delta[d\text{BR}_{\ell\ell}(\hat{s})/d\hat{s}]$  — the differential BR normalized to the partial NNLO result — where we have sequentially included the corrections listed above.

Including the main parametric uncertainties, our final result reads

$$\text{BR}_{\ell\ell}(0.05 \leq \hat{s} \leq 0.25) = \tag{26}$$

$$\left[1.442 \pm_{0.092}^{0.098} |M_t \pm_{0.069}^{0.054} |_{\text{scale}} \pm 0.041_C \pm 0.032_{\text{BR}_{sl}} \pm_{0.009}^{0.001} |_{m_c} \pm 0.002_{m_b}\right] \times 10^{-6}.$$

Here the whole dependence on  $\lambda_1$  is absorbed into the factor  $C$ . As already in the case of  $C$ , we neglect effects suppressed by three powers of the heavy quark masses in  $\bar{B} \rightarrow X_s \ell^+ \ell^-$  [33], which in the low- $\hat{s}$  region should not exceed 2% anyway. The uncertainty related to the CKM matrix elements is below 1%. To be conservative, one could also consider an additional 2% uncertainty due to unknown electroweak effects. Combining in quadrature all uncertainties given in Eq.(26) with the latter three, the total error is about 9%, very similar to the one for inclusive radiative decays [25].

Though useful for comparison with previous analyses [4], the BR integrated in the region  $0.05 \leq \hat{s} \leq 0.25$  is an idealization. A quantity closer to experiment is the BR integrated in the region  $1 \text{ GeV}^2 \leq q^2 \leq 6 \text{ GeV}^2$  [5]. The results for the integrated BR employing this range are given in the second line of Table 2 together with their scale dependence. Unfortunately, the choice of the integration variable introduces an enhanced dependence on the bottom quark mass. In our calculation we have employed the  $b$ -quark pole mass, which is subject to a much larger uncertainty than an appropriate short-distance  $b$ -quark mass. For example the  $1S$  or the kinetic low-energy  $b$ -quark mass [27] are known to better than 50 MeV. Our final result is

$$\text{BR}_{\ell\ell}(1 \text{ GeV}^2 \leq q^2 \leq 6 \text{ GeV}^2) = \tag{27}$$

$$\left[1.574 \pm_{0.100}^{0.106} |M_t \pm_{0.067}^{0.072} |_{m_b} \pm_{0.075}^{0.059} |_{\text{scale}} \pm 0.045_C \pm 0.035_{\text{BR}_{sl}} \pm_{0.013}^{0.001} |_{m_c}\right] \times 10^{-6}.$$

The total error is about 10% and is again dominated by the uncertainty on the top quark mass, which will soon be reduced by a factor of two by CDF and D0 at the Tevatron. Moreover, the substantial error from the  $b$ -quark mass is an artifact of the employed scheme, which can be reduced by a factor of three or even more by changing the renormalization scheme of the  $b$ -quark mass. Hence it should not be interpreted as a limitation.

For what concerns the FB asymmetry, we have investigated the impact of the choice of normalization and of the electroweak corrections on the so-called unnormalized asymmetry defined as in [4]

$$A_{\text{FB}}(\hat{s}) = \frac{\text{BR}[\bar{B} \rightarrow X_c \ell \nu]}{\Gamma[\bar{B} \rightarrow X_c \ell \nu]} \int_{-1}^1 d \cos \theta_\ell \frac{d^2 \Gamma[\bar{B} \rightarrow X_s \ell^+ \ell^-]}{d\hat{s} d \cos \theta_\ell} \text{sgn}(\cos \theta_\ell), \tag{28}$$

	$\hat{s}_0$ without $O(1/m_{b,c}^2)$	$\hat{s}_0$ with $O(1/m_{b,c}^2)$
unexpanded $A_{\text{FB}}(\hat{s})$ as in (28)	$0.160_{-0.005}^{+0.008}$	$0.167_{-0.006}^{+0.008}$
expanded $A_{\text{FB}}(\hat{s})$ as in (30)	$0.151_{-0.004}^{+0.005}$	$0.156_{-0.005}^{+0.005}$
expanded $\bar{A}_{\text{FB}}(\hat{s})$ as in (31)	$0.157_{-0.009}^{+0.005}$	$0.163_{-0.010}^{+0.007}$
unexpanded $A_{\text{FB}}(\hat{s})$ as in (28) + EW	$0.164_{-0.004}^{+0.004}$	$0.170_{-0.005}^{+0.004}$
expanded $A_{\text{FB}}(\hat{s})$ as in (30) + EW	$0.154_{-0.004}^{+0.004}$	$0.159_{-0.004}^{+0.004}$
expanded $\bar{A}_{\text{FB}}(\hat{s})$ as in (31) + EW	$0.160_{-0.009}^{+0.006}$	$0.166_{-0.010}^{+0.007}$

Table 3: Zero of FB asymmetry before and after the inclusion of  $1/m_b^2$  and  $1/m_c^2$  power corrections.

where

$$\int_{-1}^1 d \cos \theta_\ell \frac{d^2 \Gamma[\bar{B} \rightarrow X_s \ell^+ \ell^-]}{d \hat{s} d \cos \theta_\ell} \text{sgn}(\cos \theta_\ell) = \frac{G_\mu^2 m_{b,\text{pole}}^5 |V_{ts}^* V_{tb}|^2}{48 \pi^3} \left( \frac{\alpha(m_b)}{4 \pi} \right)^2 (1 - \hat{s})^2 \times \left\{ -6 \text{Re} \left( \tilde{C}_{7,\text{FB}}^{\text{eff}}(\hat{s}) \tilde{C}_{10,\text{FB}}^{\text{eff}}(\hat{s})^* \right) - 3 \hat{s} \text{Re} \left( \tilde{C}_{9,\text{FB}}^{\text{eff}}(\hat{s}) \tilde{C}_{10,\text{FB}}^{\text{eff}}(\hat{s})^* \right) + A_{\text{FB}}^{\text{Brems}}(\hat{s}) \right\}, \quad (29)$$

and the effective Wilson coefficients include all real and virtual corrections calculated in [4] as indicated by the subscript FB. The last term of Eq. (29) encodes finite bremsstrahlungs corrections evaluated in the last reference of [4] which we have not included<sup>6</sup>. At  $O(\alpha)$  the definition of the effective Wilson coefficients is affected by the presence of the electroweak penguin operators  $Q_3^Q - Q_6^Q$  and of  $Q_1^b$  — for a detailed discussion we again refer to [22].

Implementing all the relevant NNLO QCD corrections we obtain for the position of the zero of the unnormalized FB asymmetry (28) the values given in the first column of the first line of Table 3, in agreement with [4, 8]. While in Refs. [4, 8] only the low-energy renormalization scale was varied, the errors in Table 3 also include the matching scale dependence.

Since the position of the zero of the FB asymmetry is known to be especially sensitive to physics beyond the SM, a comprehensive study of the residual theoretical error attached to it is important. In order to get a grasp for the size of higher order corrections, we consider the normalization to the charmless semileptonic decay rate

$$A_{\text{FB}}(\hat{s}) = \frac{\text{BR}[\bar{B} \rightarrow X_c \ell \nu]}{\Gamma[\bar{B} \rightarrow X_u \ell \nu]} \frac{1}{C} \left| \frac{V_{ub}}{V_{cb}} \right|^2 \int_{-1}^1 d \cos \theta_\ell \frac{d^2 \Gamma[\bar{B} \rightarrow X_s \ell^+ \ell^-]}{d \hat{s} d \cos \theta_\ell} \text{sgn}(\cos \theta_\ell), \quad (30)$$

in combination with  $C$  and perform an expansion of the ratio of Eq. (30) in  $\alpha_s$  to improve the convergence of the perturbative series. The corresponding result is displayed in the

<sup>6</sup>These corrections turn out to be below 1%.

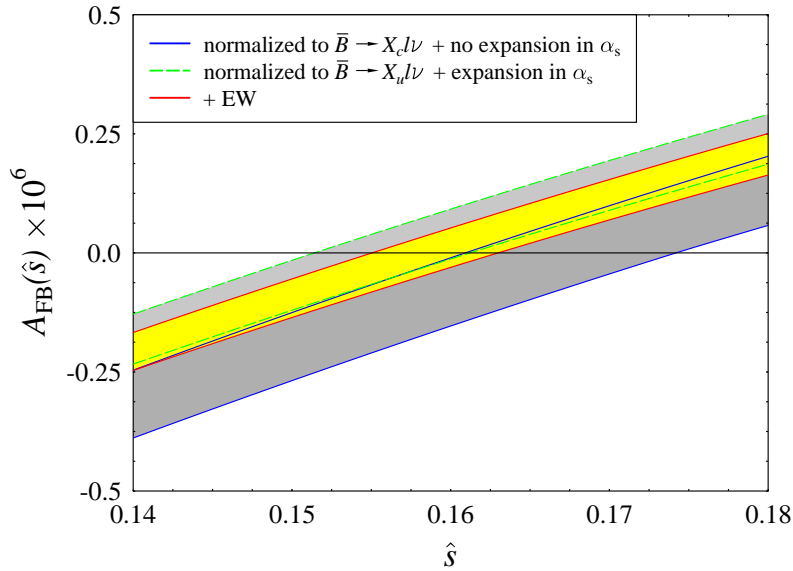


Figure 6: Unnormalized FB asymmetry  $A_{\text{FB}}(\hat{s})$  in the low- $\hat{s}$  region including  $1/m_b^2$  and  $1/m_c^2$  power corrections. Compared is the NNLO QCD result for the normalization given in Eq. (28) and the one given in Eq. (30) performing a subsequent expansion in  $\alpha_s$ . Furthermore we also display the result of Eq. (30) after the inclusion of electroweak effects (central yellow band).

first entry of the second line of Table 3. Note that in this case the numerical value obtained for  $\hat{s}_0$  does *no longer* correspond to the zero of the curly bracket in Eq. (29). The difference between the values of  $\hat{s}_0$  in the first and second line of Table 3 is obviously due to different higher order terms and can give an indication of the residual theoretical error.

We also consider the so-called normalized FB asymmetry, which is certainly a quantity closer to experiment:

$$\bar{A}_{\text{FB}}(\hat{s}) = \frac{1}{d\Gamma[\bar{B} \rightarrow X_s l^+ l^-]/d\hat{s}} \int_{-1}^1 d \cos \theta_\ell \frac{d^2\Gamma[\bar{B} \rightarrow X_s l^+ l^-]}{d\hat{s} d \cos \theta_\ell} \text{sgn}(\cos \theta_\ell). \quad (31)$$

Given the small value of the LO term of  $d\Gamma[\bar{B} \rightarrow X_s l^+ l^-]/d\hat{s}$ , a naive  $\alpha_s$  expansion of this ratio is problematic. However, the  $\alpha_s$  expansion converges reasonably well if the perturbative expansion is reorganized following the first paper of [4], namely absorbing  $C_{s,9}^{(0)}(\mu_b)$  into  $C_{s,9}^{(1)}(\mu_b)$ . With respect to the unexpanded form, which obviously reproduces the value given in the first column of the first line of Table 3, the zero is shifted toward lower values, as can be seen by comparing the first and the third entry in the first column of that table. Finally, the next three entries of the first column of Table 3 correspond to the results for  $\hat{s}_0$  in the three approaches described above after the inclusion of the electroweak effects.

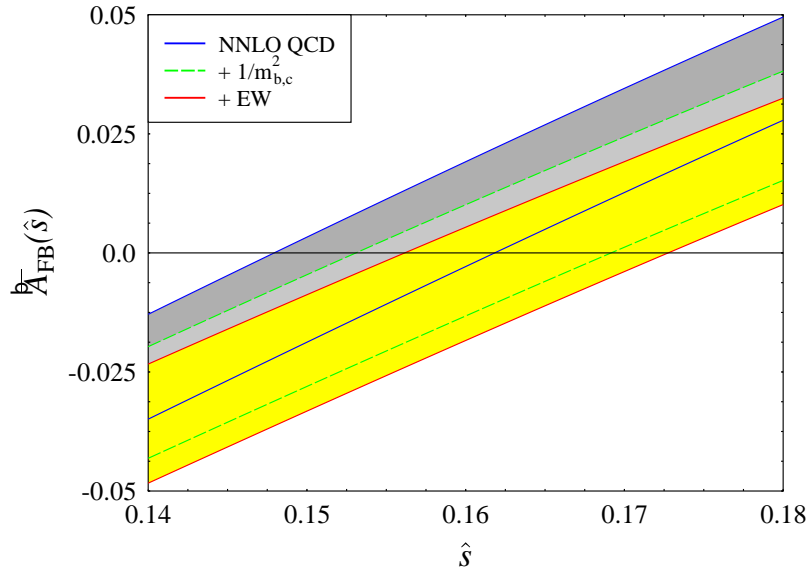


Figure 7: Normalized FB asymmetry  $\bar{A}_{\text{FB}}(\hat{s})$  in the low- $\hat{s}$  region in the NNLO QCD approximation as given in Eq. (31) without expansion in  $\alpha_s$ . Furthermore the effects of including power corrections (central band) and higher order electroweak effects (lower yellow band) are shown.

Unlike previous analyses, we also include power corrections of  $O(1/m_b^2)$  [29] and  $O(1/m_c^2)$  [30] in the computation of the zero of the FB asymmetry. In doing so we always expand the asymmetry in powers of the heavy quark masses. The corresponding numerical values for  $\hat{s}_0$  can be found in the second column of Table 3. Comparing the results in that table, one observes that higher order electroweak effects amount to around +2%, independent on which normalization is used and on whether an expansion in  $\alpha_s$  is performed or not. The  $O(1/m_b^2)$  and  $O(1/m_c^2)$  corrections turn out to be at the level of +4%. The unnormalized FB asymmetry  $A_{\text{FB}}(\hat{s})$  calculated in the two above approaches in the vicinity of the zero is shown in Figure 6, whereas in Figure 7 we plot the unexpanded  $\bar{A}_{\text{FB}}(\hat{s})$ , showing the importance of the power and electroweak corrections.

A glance at Table 3 and Figures 6 and 7 shows that the dependence of the zero on the specific method used to calculate it is generally larger than the scale dependence associated with it. This suggests that the observed scale dependence alone does *not* provide a reasonable estimate of higher order QCD and electroweak corrections, as pointed out already in the third paper of [4]. Following a reasoning similar as for  $\text{BR}_{\ell\ell}$ , we adopt as the central value for  $\hat{s}_0$  the average of the two expanded results in Table 3 and assign to it a rather conservative total error of 6%, that covers the whole range of possible values:

$$\hat{s}_0 = 0.163 \pm 0.010_{\text{theory}}. \quad (32)$$

The uncertainties due to  $M_t$  and the non-perturbative parameters  $\lambda_1$  and  $\lambda_2$  are at the 0.1%

level or less. Converting this result into a value of  $q^2$  introduces again a large uncertainty due to the bottom quark mass. We find

$$q_0^2 = (3.76 \pm 0.22_{\text{theory}} \pm 0.24_{m_b}) \text{ GeV}^2, \quad (33)$$

with a total error close to 9%. However, also in this case the error due to the  $b$ -quark mass can be drastically reduced by performing the calculation in a different mass scheme.

## 5 Summary

Rare semileptonic  $B$  decays are going to play an important role in the search for new physics at the  $B$  factories and upcoming flavor physics experiments at the Tevatron and the LHC. From the theoretical point of view the inclusive mode at low  $q^2$  is particular interesting, since it can be accurately computed in the SM. In this paper we have first completed the NNLO QCD analysis of  $\bar{B} \rightarrow X_s \ell^+ \ell^-$  with the calculation of the last two missing components, and then discussed electroweak effects. The new NNLO QCD contributions are relatively small — they amount to around +1% and −4% — and tend to partially cancel each other. Our treatment of electroweak effects is complete only for what concerns the leading logarithms of photonic origin but, pending an exhaustive investigation of the missing matrix elements [22, 24], we expect it to capture all the dominant contributions. The impact of electroweak effects depends on the scale employed for  $\alpha(\mu)$  in the prefactor for  $\text{BR}_{\ell\ell}$ . As a result of accidental cancellations, they change the value of the low-energy BR by only −1.5% for  $\mu = O(m_b)$ , while if one adopts  $\mu = O(M_w)$  the effect is much more relevant, about −8.5%. Our calculation drastically reduces the large uncertainty of almost 8% related to higher order electroweak effects, which has affected previous analyses. We have also calculated the FB asymmetry. The location of its zero is shifted by approximately +2% due to the electroweak corrections.

We have also introduced a few improvements in the calculation of the decay rate in the region of low dilepton invariant masses, aimed at reducing the theoretical error. After a careful study of the various sources of uncertainty, we estimate a 9% to 10% error on our result for the BR in the  $\hat{s} = 0.05 - 0.25$  or  $q^2 = 1 - 6 \text{ GeV}^2$  window, the dominant source of which is the uncertainty on the top quark mass. For what concerns the zero of the FB asymmetry, our estimate for the residual uncertainty is 6% to 9%.

## Acknowledgments

During the final stage of our work we have become aware of an ongoing analysis [24] of electroweak effects in  $\bar{B} \rightarrow X_s \ell^+ \ell^-$  that overlaps in part with Section 3 of this paper. We are grateful to Mikolaj Misiak for very informative discussions, for reading carefully a preliminary version of our manuscript, and for reminding us of the role of  $Q_1^b$ . We would also like to thank Andrzej Buras and Gino Isidori for many useful discussions.

The work of C. B. was supported by the *Deutsche Forschungsgemeinschaft* (DFG) under contract Bu.706/1-2 and by the G.I.F Grant No. G-698-22.7/2001, and in part by the U.S. Department of Energy under contract No. DOE-FG03-97ER40546. The work of M. G. was supported by the *Deutsches Bundesministerium für Bildung und Forschung* under the contract No. 05HT1WOA3. The work of P. G. is supported by a Marie Curie Fellowship, contract No. HPMF-CT-2000-01048. Finally, the work of U. H. is supported by the U.S. Department of Energy under contract No. DE-AC02-76CH03000.

## Appendix

We report below the complete  $O(\alpha_s)$ ,  $O(\alpha_s^2)$ ,  $O(\alpha)$  and  $O(\alpha\alpha_s)$  ADMs making explicit their dependence on the coefficients of the QED and QCD  $\beta$  function:

$$\beta_s = -\frac{g_s^3}{16\pi^2} \left( \beta_s^{(0)} + \frac{g_s^2}{16\pi^2} \beta_s^{(1)} + \frac{e^2}{16\pi^2} \beta_{se}^{(1)} \right), \quad \beta_e = \frac{e^3}{16\pi^2} \left( \beta_e^{(0)} + \frac{g_s^2}{16\pi^2} \beta_{es}^{(1)} \right). \quad (34)$$

For five active quark and three active lepton flavors the values of the  $\overline{\text{MS}}$   $\beta$  coefficients are

$$\beta_s^{(0)} = \frac{23}{3}, \quad \beta_s^{(1)} = \frac{116}{3}, \quad \beta_{se}^{(1)} = -\frac{22}{9}, \quad \beta_e^{(0)} = \frac{80}{9}, \quad \beta_{es}^{(1)} = \frac{176}{9}. \quad (35)$$

Adopting the ordering of operators as introduced in Eq. (1) the matrices  $\hat{\gamma}_s^{(0)}$  and  $\hat{\gamma}_s^{(1)}$  take the following form

$$\hat{\gamma}_s^{(0)} = \begin{pmatrix} -4 \frac{8}{3} & 0 & -\frac{2}{9} & 0 & 0 & 0 & 0 & 0 & 0 & 0 & 0 & 0 & -\frac{32}{27} & 0 \\ 12 & 0 & 0 & \frac{4}{3} & 0 & 0 & 0 & 0 & 0 & 0 & 0 & 0 & -\frac{8}{9} & 0 \\ 0 & 0 & 0 & -\frac{52}{3} & 0 & 2 & 0 & 0 & 0 & 0 & 0 & 0 & -\frac{16}{9} & 0 \\ 0 & 0 & -\frac{40}{9} & -\frac{100}{9} & \frac{4}{9} & \frac{5}{6} & 0 & 0 & 0 & 0 & 0 & 0 & \frac{32}{27} & 0 \\ 0 & 0 & 0 & -\frac{256}{3} & 0 & 20 & 0 & 0 & 0 & 0 & 0 & 0 & -\frac{112}{9} & 0 \\ 0 & 0 & -\frac{256}{9} & \frac{56}{9} & \frac{40}{9} & -\frac{2}{3} & 0 & 0 & 0 & 0 & 0 & 0 & \frac{512}{27} & 0 \\ 0 & 0 & 0 & -\frac{8}{9} & 0 & 0 & 0 & -20 & 0 & 2 & 0 & 0 & -\frac{272}{27} & 0 \\ 0 & 0 & 0 & \frac{16}{27} & 0 & 0 & -\frac{40}{9} & -\frac{52}{3} & \frac{4}{9} & \frac{5}{6} & 0 & 0 & -\frac{32}{81} & 0 \\ 0 & 0 & 0 & -\frac{128}{9} & 0 & 0 & 0 & -128 & 0 & 20 & 0 & 0 & -\frac{2768}{27} & 0 \\ 0 & 0 & 0 & \frac{184}{27} & 0 & 0 & -\frac{256}{9} & -\frac{160}{3} & \frac{40}{9} & -\frac{2}{3} & 0 & 0 & -\frac{512}{81} & 0 \\ 0 & 0 & 0 & \frac{4}{3} & 0 & 0 & 0 & 0 & 0 & 0 & 4 & 0 & \frac{16}{9} & 0 \\ 0 & 0 & 0 & 0 & 0 & 0 & 0 & 0 & 0 & 0 & 0 & \frac{32}{3} - 2\beta_s^{(0)} & 0 & 0 \\ 0 & 0 & 0 & 0 & 0 & 0 & 0 & 0 & 0 & 0 & 0 & -\frac{32}{9} & \frac{28}{3} - 2\beta_s^{(0)} & 0 \\ 0 & 0 & 0 & 0 & 0 & 0 & 0 & 0 & 0 & 0 & 0 & 0 & -2\beta_s^{(0)} & 0 \\ 0 & 0 & 0 & 0 & 0 & 0 & 0 & 0 & 0 & 0 & 0 & 0 & 0 & -2\beta_s^{(0)} \end{pmatrix}, \quad (36)$$

$$\hat{\gamma}_s^{(1)} = \begin{pmatrix} -\frac{355}{9} & -\frac{502}{27} & -\frac{1412}{243} & -\frac{1369}{243} & \frac{134}{243} & -\frac{35}{162} & 0 & 0 & 0 & 0 & 0 & -\frac{232}{243} & \frac{167}{162} & -\frac{2272}{729} & 0 \\ -\frac{35}{3} & -\frac{28}{3} & -\frac{416}{81} & \frac{1280}{81} & \frac{56}{81} & \frac{35}{27} & 0 & 0 & 0 & 0 & 0 & \frac{464}{81} & \frac{76}{27} & \frac{1952}{243} & 0 \\ 0 & 0 & -\frac{4468}{81} & -\frac{31469}{81} & \frac{400}{81} & \frac{3373}{108} & 0 & 0 & 0 & 0 & 0 & \frac{64}{81} & \frac{368}{27} & -\frac{6752}{243} & 0 \\ 0 & 0 & -\frac{8158}{243} & -\frac{59399}{243} & \frac{269}{486} & \frac{12899}{648} & 0 & 0 & 0 & 0 & 0 & -\frac{200}{243} & -\frac{1409}{162} & -\frac{2192}{729} & 0 \\ 0 & 0 & -\frac{251680}{81} & -\frac{128648}{81} & \frac{23836}{81} & \frac{6106}{27} & 0 & 0 & 0 & 0 & 0 & -\frac{6464}{27} & \frac{13052}{27} & -\frac{84032}{243} & 0 \\ 0 & 0 & \frac{58640}{243} & -\frac{26348}{243} & -\frac{14324}{243} & -\frac{2551}{162} & 0 & 0 & 0 & 0 & 0 & -\frac{11408}{243} & -\frac{2740}{81} & -\frac{37856}{729} & 0 \\ 0 & 0 & \frac{832}{243} & -\frac{4000}{243} & -\frac{112}{243} & -\frac{70}{81} & -\frac{404}{9} & -\frac{3077}{9} & \frac{32}{9} & \frac{1031}{36} & 0 & -\frac{64}{243} & -\frac{368}{81} & -\frac{24352}{729} & 0 \\ 0 & 0 & \frac{3376}{729} & \frac{6344}{729} & -\frac{280}{729} & \frac{55}{486} & -\frac{2698}{81} & -\frac{8035}{27} & -\frac{49}{162} & \frac{4493}{216} & 0 & \frac{776}{729} & \frac{743}{486} & \frac{54608}{2187} & 0 \\ 0 & 0 & \frac{2272}{243} & -\frac{72088}{243} & -\frac{688}{243} & -\frac{1240}{81} & -\frac{19072}{9} & -\frac{14096}{9} & \frac{1708}{9} & \frac{1622}{9} & 0 & \frac{6464}{243} & -\frac{7220}{81} & -\frac{227008}{729} & 0 \\ 0 & 0 & \frac{45424}{729} & \frac{84236}{729} & -\frac{3880}{729} & \frac{1220}{243} & \frac{32288}{81} & -\frac{15976}{27} & -\frac{6692}{81} & -\frac{2437}{54} & 0 & \frac{63824}{729} & \frac{6700}{243} & \frac{551648}{2187} & 0 \\ 0 & 0 & -\frac{1576}{81} & \frac{446}{27} & \frac{172}{81} & \frac{40}{27} & 0 & 0 & 0 & 0 & \frac{325}{9} & -\frac{808}{81} & \frac{349}{27} & -\frac{8}{9} & 0 \\ 0 & 0 & 0 & 0 & 0 & 0 & 0 & 0 & 0 & 0 & 0 & \frac{4688}{27} & -2\beta_s^{(1)} & 0 & 0 \\ 0 & 0 & 0 & 0 & 0 & 0 & 0 & 0 & 0 & 0 & 0 & -\frac{2192}{81} & \frac{4063}{27} & -2\beta_s^{(1)} & 0 \\ 0 & 0 & 0 & 0 & 0 & 0 & 0 & 0 & 0 & 0 & 0 & 0 & 0 & -2\beta_s^{(1)} & 0 \\ 0 & 0 & 0 & 0 & 0 & 0 & 0 & 0 & 0 & 0 & 0 & 0 & 0 & 0 & -2\beta_s^{(1)} \end{pmatrix} \quad (37)$$

The one-loop  $O(\alpha_s)$  mixing of the electroweak penguin operators  $Q_3^Q-Q_6^Q$  into  $Q_9$ , as well as the mixing of  $Q_1^b$  has never been computed before. The same applies to the complete two-loop  $O(\alpha_s^2)$  mixing<sup>7</sup> of  $Q_3^Q-Q_6^Q$  and  $Q_1^b$ . As far as the remaining entries are concerned our results agree with the well-established results in the literature [3, 10, 12, 34, 36].

The matrices  $\hat{\gamma}_e^{(0)}$  and  $\hat{\gamma}_e^{(1)}$  are given by

$$\hat{\gamma}_e^{(0)} = \begin{pmatrix} -\frac{8}{3} & 0 & 0 & 0 & 0 & 0 & \frac{32}{27} & 0 & 0 & 0 & 0 & 0 & 0 & 0 & 0 \\ 0 & -\frac{8}{3} & 0 & 0 & 0 & 0 & \frac{8}{9} & 0 & 0 & 0 & 0 & 0 & 0 & 0 & 0 \\ 0 & 0 & 0 & 0 & 0 & 0 & \frac{76}{9} & 0 & -\frac{2}{3} & 0 & 0 & 0 & 0 & 0 & 0 \\ 0 & 0 & 0 & 0 & 0 & 0 & -\frac{32}{27} & \frac{20}{3} & 0 & -\frac{2}{3} & 0 & 0 & 0 & 0 & 0 \\ 0 & 0 & 0 & 0 & 0 & 0 & \frac{496}{9} & 0 & -\frac{20}{3} & 0 & 0 & 0 & 0 & 0 & 0 \\ 0 & 0 & 0 & 0 & 0 & 0 & -\frac{512}{27} & \frac{128}{3} & 0 & -\frac{20}{3} & 0 & 0 & 0 & 0 & 0 \\ 0 & 0 & \frac{40}{27} & 0 & -\frac{4}{27} & 0 & \frac{332}{27} & 0 & -\frac{2}{9} & 0 & 0 & 0 & 0 & 0 & 0 \\ 0 & 0 & 0 & \frac{40}{27} & 0 & -\frac{4}{27} & \frac{32}{81} & \frac{20}{9} & 0 & -\frac{2}{9} & 0 & 0 & 0 & 0 & 0 \\ 0 & 0 & \frac{256}{27} & 0 & -\frac{40}{27} & 0 & \frac{3152}{27} & 0 & -\frac{20}{9} & 0 & 0 & 0 & 0 & 0 & 0 \\ 0 & 0 & 0 & \frac{256}{27} & 0 & -\frac{40}{27} & \frac{512}{81} & \frac{128}{9} & 0 & -\frac{20}{9} & 0 & 0 & 0 & 0 & 0 \\ 0 & 0 & 0 & 0 & 0 & 0 & -\frac{16}{9} & 0 & 0 & 0 & \frac{4}{3} & 0 & 0 & 0 & 0 \\ 0 & 0 & 0 & 0 & 0 & 0 & 0 & 0 & 0 & 0 & 0 & \frac{16}{9} & -\frac{8}{3} & 0 & 0 \\ 0 & 0 & 0 & 0 & 0 & 0 & 0 & 0 & 0 & 0 & 0 & 0 & \frac{8}{9} & 0 & 0 \\ 0 & 0 & 0 & 0 & 0 & 0 & 0 & 0 & 0 & 0 & 0 & 0 & 0 & 8-2\beta_e^{(0)} & -4 \\ 0 & 0 & 0 & 0 & 0 & 0 & 0 & 0 & 0 & 0 & 0 & 0 & 0 & -4 & -2\beta_e^{(0)} \end{pmatrix}, \quad (38)$$

<sup>7</sup>The self-mixing of  $Q_3^Q-Q_6^Q$  has been computed in the so-called ‘‘standard’’ operator basis in [35]. Since the operator basis of the latter papers differs from the one used here one has to perform a non-trivial transformation. This can serve as a cross-check of the direct calculation. See Ref. [22] for details.



$$\hat{\gamma}_e^{(1)} = \begin{pmatrix} \frac{169}{9} \frac{100}{27} & 0 & \frac{254}{729} & 0 & 0 & \frac{2272}{729} & \frac{122}{81} & 0 & \frac{49}{81} & 0 & -\frac{928}{729} & \frac{118}{243} & -\frac{11680}{2187} & -\frac{416}{81} \\ \frac{50}{3} - \frac{8}{3} & 0 & \frac{1076}{243} & 0 & 0 & -\frac{1952}{243} & -\frac{748}{27} & 0 & \frac{82}{27} & 0 & -\frac{232}{243} & -\frac{92}{81} & -\frac{2920}{729} & -\frac{104}{27} \\ 0 & 0 & 0 & \frac{11116}{243} & 0 & -\frac{14}{3} & -\frac{23488}{243} & \frac{6280}{27} & \frac{112}{9} & -\frac{538}{27} & 0 & -\frac{32}{243} & \frac{32}{81} & -\frac{39752}{729} & -\frac{136}{27} \\ 0 & 0 & \frac{280}{27} & \frac{18763}{729} & -\frac{28}{27} & -\frac{35}{18} & \frac{31568}{729} & \frac{9481}{81} & -\frac{92}{27} & -\frac{1012}{81} & 0 & \frac{64}{729} & \frac{260}{243} & \frac{1024}{2187} & -\frac{448}{81} \\ 0 & 0 & 0 & \frac{111136}{243} & 0 & -\frac{140}{3} & -\frac{233920}{243} & \frac{68848}{27} & \frac{1120}{9} & -\frac{5056}{27} & 0 & -\frac{23480}{243} & \frac{2096}{81} & -\frac{381344}{729} & -\frac{15616}{27} \\ 0 & 0 & \frac{2944}{27} & \frac{193312}{729} & -\frac{280}{27} & -\frac{175}{9} & \frac{352352}{729} & \frac{116680}{81} & -\frac{752}{27} & -\frac{10147}{81} & 0 & -\frac{6464}{729} & \frac{3548}{243} & \frac{24832}{2187} & -\frac{7936}{81} \\ 0 & 0 & -\frac{2240}{81} & \frac{39392}{729} & \frac{224}{81} & -\frac{92}{27} & -\frac{5888}{729} & \frac{13916}{81} & \frac{112}{27} & -\frac{812}{81} & 0 & -\frac{544}{729} & \frac{544}{243} & -\frac{90424}{2187} & -\frac{152}{81} \\ 0 & 0 & \frac{2176}{243} & \frac{84890}{2187} & -\frac{184}{243} & -\frac{224}{81} & -\frac{2552}{2187} & \frac{15638}{243} & -\frac{176}{81} & -\frac{2881}{486} & 0 & -\frac{64}{2187} & -\frac{260}{729} & -\frac{1024}{6561} & \frac{448}{243} \\ 0 & 0 & -\frac{23552}{81} & \frac{399776}{729} & \frac{2240}{81} & -\frac{752}{27} & -\frac{90944}{729} & \frac{90128}{81} & \frac{1120}{27} & -\frac{1748}{81} & 0 & -\frac{28936}{729} & \frac{3664}{243} & -\frac{910048}{2187} & -\frac{8000}{81} \\ 0 & 0 & \frac{23296}{243} & \frac{933776}{2187} & -\frac{1504}{243} & -\frac{2030}{81} & \frac{1312}{2187} & \frac{102488}{243} & -\frac{1592}{81} & -\frac{6008}{243} & 0 & \frac{6464}{2187} & -\frac{15212}{729} & -\frac{24832}{6561} & \frac{7936}{243} \\ 0 & 0 & 0 & -\frac{232}{81} & 0 & 0 & 0 & \frac{580}{27} & 0 & -\frac{94}{27} & -\frac{388}{9} & -\frac{232}{243} & \frac{70}{81} & \frac{344}{243} & -\frac{232}{27} \\ 0 & 0 & 0 & 0 & 0 & 0 & 0 & 0 & 0 & 0 & 0 & -\frac{256}{27} - 2\beta_{se}^{(1)} & -\frac{52}{9} & 0 & 0 \\ 0 & 0 & 0 & 0 & 0 & 0 & 0 & 0 & 0 & 0 & 0 & \frac{128}{81} & -\frac{40}{27} - 2\beta_{se}^{(1)} & 0 & 0 \\ 0 & 0 & 0 & 0 & 0 & 0 & 0 & 0 & 0 & 0 & 0 & 0 & 0 & -2\beta_{se}^{(1)} - 2\beta_{es}^{(1)} & 16 \\ 0 & 0 & 0 & 0 & 0 & 0 & 0 & 0 & 0 & 0 & 0 & 0 & 0 & 16 & -2\beta_{se}^{(1)} - 2\beta_{es}^{(1)} \end{pmatrix}. \quad (39)$$

In  $\hat{\gamma}_e^{(0)}$  only the entries corresponding to the self-mixing of  $Q_9$  and  $Q_{10}$  are new, while all other elements agree with those of [10]. On the other hand,  $\hat{\gamma}_e^{(1)}$  is entirely new.

The two-loop ADMs  $\hat{\gamma}_s^{(1)}$  and  $\hat{\gamma}_e^{(1)}$  depend on the definition of evanescent operators. We have followed the definition employed in [12, 34] extending it to include all electroweak and semileptonic operators:

$$\begin{aligned} E_1 &= (\bar{s}_L \gamma_\mu \gamma_\nu \gamma_\rho T^a c_L) (\bar{c}_L \gamma^\mu \gamma^\nu \gamma^\rho T^a b_L) - 16Q_1, \\ E_2 &= (\bar{s}_L \gamma_\mu \gamma_\nu \gamma_\rho c_L) (\bar{c}_L \gamma^\mu \gamma^\nu \gamma^\rho b_L) - 16Q_2, \\ E_3 &= (\bar{s}_L \gamma_\mu \gamma_\nu \gamma_\rho \gamma_\sigma \gamma_\tau b_L) \sum_q (\bar{q} \gamma^\mu \gamma^\nu \gamma^\rho \gamma^\sigma \gamma^\tau q) + 64Q_3 - 20Q_5, \\ E_4 &= (\bar{s}_L \gamma_\mu \gamma_\nu \gamma_\rho \gamma_\sigma \gamma_\tau T^a b_L) \sum_q (\bar{q} \gamma^\mu \gamma^\nu \gamma^\rho \gamma^\sigma \gamma^\tau T^a q) + 64Q_4 - 20Q_6, \\ E_3^Q &= (\bar{s}_L \gamma_\mu \gamma_\nu \gamma_\rho \gamma_\sigma \gamma_\tau b_L) \sum_q Q_q (\bar{q} \gamma^\mu \gamma^\nu \gamma^\rho \gamma^\sigma \gamma^\tau q) + 64Q_3^Q - 20Q_5^Q, \\ E_4^Q &= (\bar{s}_L \gamma_\mu \gamma_\nu \gamma_\rho \gamma_\sigma \gamma_\tau T^a b_L) \sum_q Q_q (\bar{q} \gamma^\mu \gamma^\nu \gamma^\rho \gamma^\sigma \gamma^\tau T^a q) + 64Q_4^Q - 20Q_6^Q, \\ E_1^b &= \frac{1}{12} (\bar{s}_L \gamma_\mu \gamma_\nu \gamma_\rho \gamma_\sigma \gamma_\tau T^a b_L) (\bar{b} \gamma^\mu \gamma^\nu \gamma^\rho \gamma^\sigma \gamma^\tau T^a b) + \frac{10}{3} (\bar{s}_L \gamma_\mu T^a b_L) (\bar{b} \gamma^\mu T^a b) \\ &\quad - \frac{7}{6} (\bar{s}_L \gamma_\mu \gamma_\nu \gamma_\rho T^a b_L) (\bar{b} \gamma^\mu \gamma^\nu \gamma^\rho T^a b) - 2Q_1^b, \\ E_2^b &= (\bar{s}_L \gamma_\mu \gamma_\nu \gamma_\rho \gamma_\sigma \gamma_\tau b_L) (\bar{b} \gamma^\mu \gamma^\nu \gamma^\rho \gamma^\sigma \gamma^\tau b) - \frac{64}{3} (\bar{s}_L \gamma_\mu b_L) (\bar{b} \gamma^\mu b) \\ &\quad + \frac{4}{3} (\bar{s}_L \gamma_\mu \gamma_\nu \gamma_\rho b_L) (\bar{b} \gamma^\mu \gamma^\nu \gamma^\rho b) - 256Q_1^b, \\ E_9 &= \frac{e^2}{g_s^2} (\bar{s}_L \gamma_\mu \gamma_\nu \gamma_\rho b_L) \sum_\ell (\bar{\ell} \gamma^\mu \gamma^\nu \gamma^\rho \ell) - 10Q_9 + 6Q_{10}, \\ E_{10} &= \frac{e^2}{g_s^2} (\bar{s}_L \gamma_\mu \gamma_\nu \gamma_\rho b_L) \sum_\ell (\bar{\ell} \gamma^\mu \gamma^\nu \gamma^\rho \gamma_5 \ell) + 6Q_9 - 10Q_{10}. \end{aligned} \quad (40)$$

At this point a comment concerning the two-loop mixing of  $Q_1^b$  is in order. Using the

definition of  $Q_1^b$ ,  $E_1^b$  and  $E_2^b$  as given in Eqs. (1) and (40), the electromagnetic operator  $Q_1^b$  mixes into new physical operators beyond the one-loop level. Needless to say, such a mixing does not alter the results presented throughout the paper. Further details on the two-loop mixing of  $Q_1^b$  will be given in a forthcoming publication [22].

## References

- [1] K. Abe *et al.* [Belle Collaboration], Phys. Rev. Lett. **88** (2002) 021801 [hep-ex/0109026]; B. Aubert *et al.* [BaBar Collaboration] Phys. Rev. Lett. **88** (2002) 241801 [hep-ex/0201008].
- [2] J. Kaneko *et al.* [Belle Collaboration], Phys. Rev. Lett. **90**, 021801 (2003) [hep-ex/0208029]; B. Aubert *et al.* [BaBar Collaboration], hep-ex/0308016.
- [3] C. Bobeth, M. Misiak and J. Urban, Nucl. Phys. **B574** (2000) 291 [hep-ph/9910220]. See references therein for a comprehensive list of earlier papers.
- [4] H. H. Asatryan *et al.*, Phys. Rev. **D65** (2002) 074004 [hep-ph/0109140]; H. H. Asatryan *et al.*, Phys. Rev. **D66** (2002) 034009 [hep-ph/0204341]; A. Ghinculov *et al.*, Nucl. Phys. **B648** (2003) 254 [hep-ph/0208088]; H. M. Asatrian *et al.*, Phys. Rev. **D66** (2002) 094013 [hep-ph/0209006]; H. M. Asatrian *et al.*, hep-ph/0311187.
- [5] A. Ghinculov *et al.*, hep-ph/0310187.
- [6] A. Ali *et al.*, Phys. Rev. **D66** (2002) 034002 [hep-ph/0112300]; G. Hiller and F. Krüger, hep-ph/0310219.
- [7] A. J. Buras *et al.*, Nucl. Phys. **B631**, 219 (2002) [hep-ph/0203135]; H. M. Asatrian, H. H. Asatryan and A. Hovhannisyan, hep-ph/0401038.
- [8] A. Ghinculov *et al.*, hep-ph/0312128.
- [9] P. Gambino and U. Haisch, JHEP **0009** (2000) 001 [hep-ph/0007259] and JHEP **0110** (2001) 020 [hep-ph/0109058]
- [10] K. Baranowski and M. Misiak, Phys. Lett. **B483** (2000) 410 [hep-ph/9907427].
- [11] A. Czarnecki and W. J. Marciano, Phys. Rev. Lett. **81** (1998) 277 [hep-ph/9804252]; A. L. Kagan and M. Neubert, Eur. Phys. J. **C7** (1999) 5 [hep-ph/9805303].
- [12] P. Gambino, M. Gorbahn and U. Haisch, Nucl. Phys. **B673** (2003) 238 [hep-ph/0306079].
- [13] P. Gambino, M. Gorbahn and U. Haisch, in preparation.
- [14] A. J. Buras *et al.*, Nucl. Phys. **B337** (1990) 313.

- [15] M. Beneke, T. Feldmann and D. Seidel, Nucl. Phys. **B612** (2001) 25 [hep-ph/0106067]; H. M. Asatrian *et al.*, hep-ph/0312063.
- [16] A. Czarnecki and K. Melnikov, Phys. Rev. Lett. **88** (2002) 131801 [hep-ph/0112264].
- [17] K. G. Chetyrkin *et al.*, Phys. Rev. **D60** (1999) 114015 [hep-ph/9906273].
- [18] P. Gambino, A. Kwiatkowski and N. Pott, Nucl. Phys. **B544** (1999) 532 [hep-ph/9810400].
- [19] See for example, G. Degrossi and A. Vicini, hep-ph/0307122. The decoupling of heavy particles, not implemented in this paper, can be readily recovered using the numerical results given in its Table 1.
- [20] A. J. Buras, M. Jamin and M. E. Lautenbacher, Nucl. Phys. **B408** (1993) 209 [hep-ph/9303284].
- [21] A. J. Buras, P. Gambino and U. Haisch, Nucl. Phys. **B570** (2000) 117 [hep-ph/9911250].
- [22] C. Bobeth *et al.*, in preparation.
- [23] G. Buchalla and A. J. Buras, Phys. Rev. **D57** (1998) 216 [hep-ph/9707243].
- [24] E. Lunghi, M. Misiak and D. Wyler, work in progress.
- [25] P. Gambino and M. Misiak, Nucl. Phys. **B611** (2001) 338 [hep-ph/0104034].
- [26] P. H. Chankowski and L. Slawianowska, hep-ph/0308032.
- [27] M. Battaglia *et al.*, hep-ph/0304132.
- [28] See <http://www.slac.stanford.edu/xorg/hfag/>.
- [29] A. F. Falk, M. E. Luke and M. J. Savage, Phys. Rev. **D49** (1994) 3367 [hep-ph/9308288]; A. Ali *et al.*, Phys. Rev. **D55** (1997) 4105 [hep-ph/9609449]; J. W. Chen, G. Rupak and M. J. Savage, Phys. Lett. **B410** (1997) 285 [hep-ph/9705219]; G. Buchalla and G. Isidori, Nucl. Phys. **B525** (1998) 333 [hep-ph/9801456].
- [30] G. Buchalla, G. Isidori and S. J. Rey, Nucl. Phys. **B511** (1998) 594 [hep-ph/9705253].
- [31] I. I. Y. Bigi *et al.*, Phys. Rev. Lett. **71** (1993) 496 [hep-ph/9304225]; A. V. Manohar and M. B. Wise, Phys. Rev. **D49** (1994) 1310 [hep-ph/9308246].
- [32] A. Sirlin, Nucl. Phys. **B196** (1982) 83.

- [33] C. W. Bauer and C. N. Burrell, Phys. Lett. **B469** (1999) 248 [hep-ph/9907517] and Phys. Rev. **D62** (2000) 114028 [hep-ph/9911404].
- [34] K. G. Chetyrkin, M. Misiak and M. Münz, Nucl. Phys. **B520** (1998) 279 [hep-ph/9711280].
- [35] A. J. Buras *et al.*, Nucl. Phys. **B400** (1993) 37 [hep-ph/9211304]; M. Ciuchini *et al.*, Nucl. Phys. **B415** (1994) 403 [hep-ph/9304257].
- [36] M. Misiak and M. Münz, Phys. Lett. **B344** (1995) 308 [hep-ph/9409454].  
K. G. Chetyrkin, M. Misiak and M. Münz, Phys. Lett. **B400** (1997) 206, Erratum-  
ibid. **B425** (1998) 414 [hep-ph/9612313].